Agrociencia Uruguay 2026 | Volume 30 | Article e1738
DOI: 10.31285/AGRO.30.1738
ISSN 2730-5066

Hydrochemical Characterization of Groundwater in the San Pedro Creek Basin and the Caballada Creek Basin, San Pedro, Colonia

Strambini, V. [1]; Collazo, P. [1]

[1] *Universidad de la República, Facultad de Ciencias, Instituto de Ciencias Geológicas, Montevideo, Uruguay*

Abstract

In the locality of San Pedro (department of Colonia, Uruguay), dairy production and agriculture are the main activities, which require considerable volumes of good-quality groundwater. The aquifers used to meet these demands are a fractured aquifer composed of Paleoproterozoic granites, and a sedimentary aquifer composed of the Raigón Formation. To assess the quality and hydrodynamic behavior of both aquifers, a survey of water points, measurements of physicochemical parameters, groundwater sampling, and generation of piezometric maps were carried out. Major-ion analyses were conducted at the Laboratorio de Agua y Suelos of the Centro Universitario Regional Litoral Norte (CENUR-LN), and arsenic analyses were carried out at the Centro Especializado en Química Toxicológica (CEQUIMTOX) of the Facultad de Química, Universidad de la República. According to the chemical analysis results, groundwater from both aquifers is classified as sodium-calcium bicarbonate type, showing high arsenic concentrations and contamination by nitrates and by total and fecal coliforms, which is primarily associated with inadequate water and soil management in dairy farming. Groundwater from the fractured and sedimentary aquifers showed an average arsenic concentration of 0.017 mg/L, with maximum concentrations of 0.034 mg/L and 0.03 mg/L, respectively. Considering both aquifers, it was found that 27% of the wells exceed the standard set by the Instituto Uruguayo de Normas Técnicas (UNIT 833:2008), and 91% of the wells exceed the concentration recommended by the World Health Organization (WHO).

Keywords: hydrochemistry, hydrogeology, Paleoproterozoic granites, Raigón Aquifer

Editor

Karina Pamoukaghlian
Universidad de la República, Facultad de Ciencias, Montevideo, Uruguay

Received *9 Apr 2025*
Accepted *15 Oct 2025*
Published *18 Jun 2026*

Correspondence

Virginia Strambini
vstrambini@fcien.edu.uy

CC BY

Strambini, V., & Collazo, P. (2026). Hydrochemical characterization of groundwater in the San Pedro Creek basin and the Caballada Creek basin, San Pedro, Colonia. *Agrociencia Uruguay, 30*, Article e1738. https://doi.org/10.31285/AGRO.30.1738

Caracterización hidroquímica de las aguas subterráneas de la cuenca del arroyo San Pedro y la cuenca del arroyo de la Caballada, San Pedro, Colonia

Resumen

En la localidad de San Pedro (departamento de Colonia, Uruguay), la producción lechera y la agricultura constituyen las principales actividades, que requieren volúmenes considerables de agua subterránea de buena calidad. Los acuíferos utilizados para satisfacer estas demandas son el acuífero fracturado, constituido por granitos Paleoproterozoicos, y el acuífero sedimentario, constituido por la Formación Raigón. Para evaluar la calidad y el comportamiento hidrodinámico de ambos acuíferos, se realizó un inventario de puntos de agua, mediciones de parámetros fisicoquímicos, muestreo de aguas subterráneas y elaboración de mapas piezométricos. Los análisis de iones mayoritarios fueron realizados por el Laboratorio de Agua y Suelos del Centro Universitario Regional Litoral Norte (CENUR-LN), y los análisis de arsénico fueron efectuados por el Centro Especializado en Química Toxicológica (CEQUIMTOX) de la Facultad de Química, Universidad de la República. Según los resultados de los análisis químicos, el agua subterránea de ambos acuíferos se clasifica como bicarbonatada sódica-cálcica, mostrando altas concentraciones de arsénico y contaminación por nitratos, coliformes totales y fecales, lo que se asocia principalmente con un manejo inadecuado del agua y del suelo en la producción lechera. Se obtuvo que el agua subterránea de los acuíferos fracturado y sedimentario presenta una concentración media de arsénico de 0,017 mg/L, con una concentración máxima de 0,034 mg/L y 0,03 mg/L, respectivamente. Considerando ambos acuíferos, se concluye que 27 % de los pozos presentan concentraciones que superan la normativa del Instituto Uruguayo de Normas Técnicas (UNIT 833:2008) y 91 % de los pozos superan la concentración sugerida por la Organización Mundial de la Salud (OMS).

Palabras clave: hidroquímica, hidrogeología, granitos Paleoproterozoicos, Acuífero Raigón

Caracterização hidroquímica das águas subterrâneas da bacia do arroio San Pedro e da bacia do arroio da Caballada, San Pedro, Colônia

Resumo

Na localidade de San Pedro (departamento de Colônia, Uruguai), a produção leitera e a agricultura constituem as principais atividades, que requerem volumes consideráveis de água subterrânea de boa qualidade. Os aquíferos utilizados para suprir essas demandas são o aquífero fraturado, constituído por granitos Paleoproterozoicos, e o aquífero sedimentar, constituído pela Formação Raigón. Para avaliar a qualidade e o comportamento hidrodinâmico de ambos os aquíferos, foi realizado um inventário de pontos de água, medições de parâmetros físico-químicos, amostragem de águas subterrâneas e elaboração de mapas piezométricos. As análises de íons majoritários foram realizadas pelo Laboratorio de Agua y Suelos do Centro Universitario Regional Litoral Norte (CENUR-LN), e as análises de arsênio foram efetuadas pelo Centro Especializado en Química Toxicológica (CEQUIMTOX) da Facultad de Química, Universidad de la República. De acordo com os resultados das análises químicas, a água subterrânea de ambos os aquíferos classifica-se como do tipo bicarbonatada sódico-cálcica, apresentando altas concentrações de arsênio e contaminação por nitratos, coliformes totais e fecais, o que se associa principalmente ao manejo inadequado da água e do solo na produção leiteira. Observou-se que a água subterrânea dos aquíferos fraturado e sedimentar apresenta uma concentração média de arsênio de 0,017 mg/L, com concentrações máximas de 0,034 mg/L e 0,03 mg/L, respectivamente. Considerando ambos os aquíferos, conclui-se que 27% dos poços apresentam concentrações que superam a norma do Instituto Uruguayo de Normas Técnicas (UNIT 833:2008) e 91% dos poços excedem a concentração recomendada pela Organização Mundial da Saúde (OMS).

Palavras-chave: hidroquímica, hidrogeologia, granitos Paleoproterozóicos, Aquífero Raigón

1. Introduction

Groundwater constitutes one of the main natural resources for the development of agricultural activities. Dairy production, one of the most relevant activities in Uruguay, can affect groundwater quality when effluent management and treatment systems are not adequately designed, with nitrate being one of the most significant contaminants.

The department of Colonia remains one of the main dairy producers in the country, where extensive rainfed agriculture and, to a lesser extent, intensive agriculture are also practiced. The study area is located in the southwestern sector of Colonia, about 18 km from the city of Colonia del Sacramento, and covers an approximate area of 150 km^2 (Figure 1). Groundwater is used for human and animal consumption, irrigation, and cleaning in dairies. Therefore, it is essential to identify the exploited aquifers and determine their use. In addition, it is necessary to characterize their physicochemical properties, such as electrical conductivity, pH, Eh, dissolved oxygen, total dissolved solids, turbidity, temperature, and total hardness, in order to manage them sustainably. Major ions were analyzed, including chloride, nitrate, bicarbonate, sulfate, sodium, potassium, magnesium, and calcium, as well as a trace element, total arsenic.

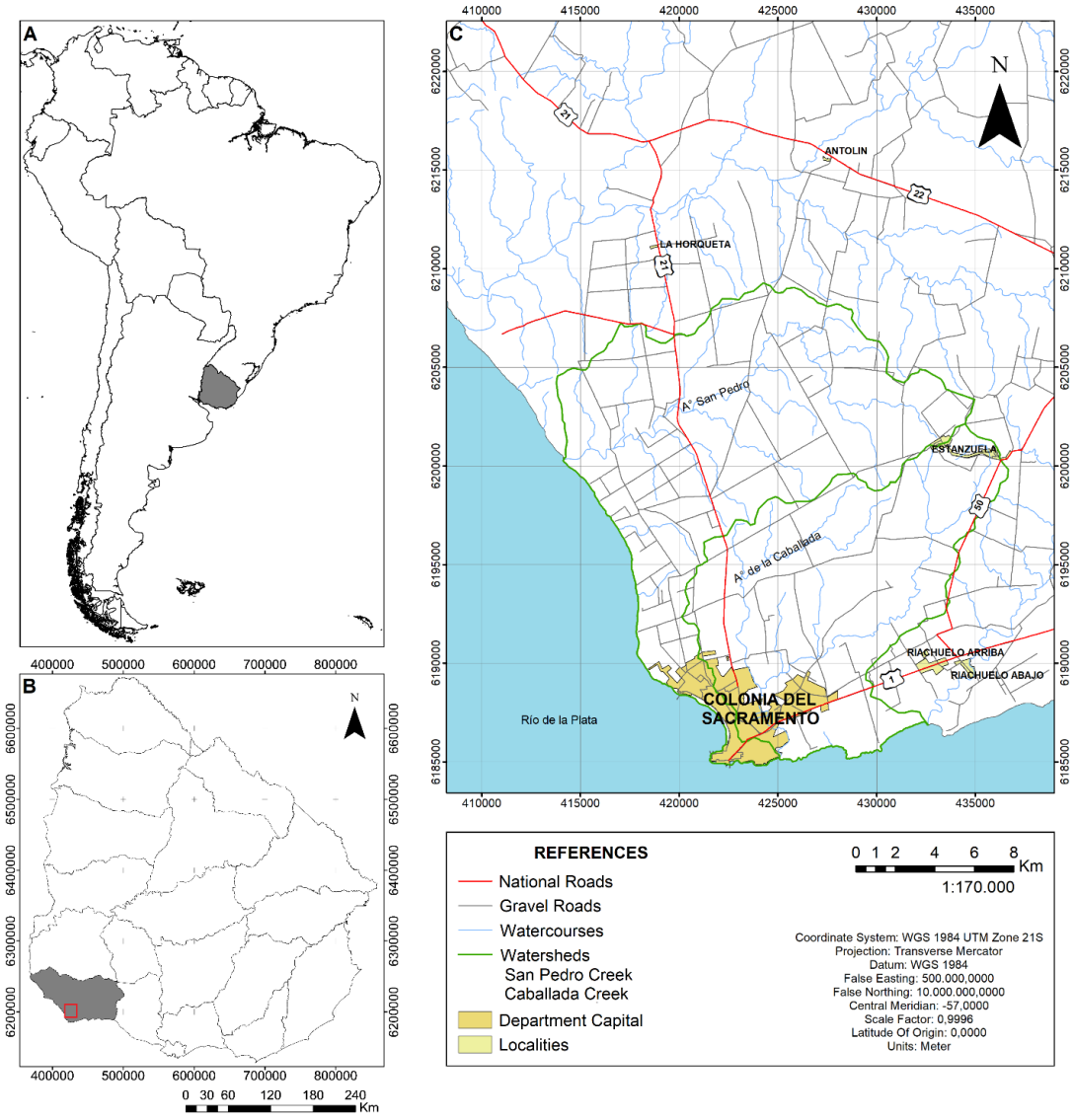

Figure 1. (A) Location of the study area in Colonia, Uruguay, South America. (B) Map of Uruguay showing the study area in Colonia (red box). (C) Detailed map of the study area

The study aims to characterize the chemistry, assess the quality, and determine the hydrodynamic behavior of the aquifers present in the San Pedro Creek and Caballada Creek basins, in the locality of San Pedro, Colonia.

The data were obtained within the framework of the undergraduate thesis “Vulnerability and Hydrogeochemical Characterization of Groundwater in the San Pedro Creek Basin and Caballada Creek Basin, San Pedro, Colonia” (Strambini Ruiz, 2023), which constituted the first study on groundwater in this region and revealed the potential health risk associated with water quality.

1.1 Geological Background

The study area is composed of Paleoproterozoic granite-gneiss belts and Cenozoic sedimentary units, represented by the Raigón and Libertad formations (Bossi & Ferrando, 2001). According to the geological map, the Fray Bentos Formation is also present in the area, although it is not considered in this study because it is not related to the objectives of this work (Figure 2). In addition, the Arroyo Minuano, Arroyo Tarariras, and Piedra Los Indios granites are recognized in the area (Gianotti & Arrighetti, 2017).

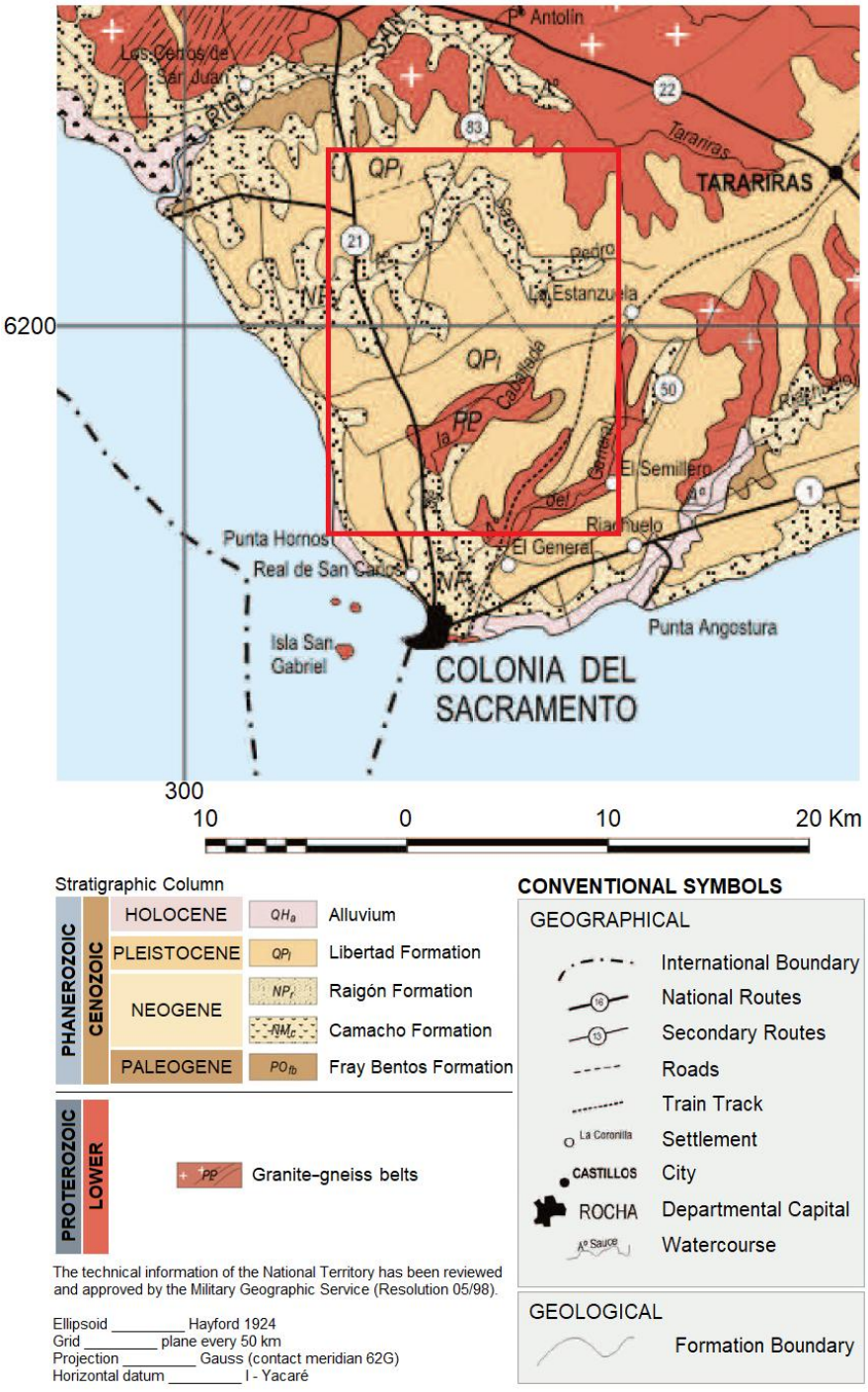

Figure 2. Section of the Geological Map of Uruguay at a scale of 1:500.000 (study area marked in red).

Source. Modified from Bossi and Ferrando (2001).

Arroyo Minuano Granite: A leucocratic, medium-grained granite, equigranular to locally inequigranular and isotropic, showing mild ductile deformation. It is composed of quartz, pink feldspar and abundant biotite. The granite is cut by numerous vertically oriented pegmatitic dikes, with a general orientation of N80E, composed of feldspar crystals up to 7-cm long (Gianotti & Arrighetti, 2017).

Arroyo Tarariras Granite: A leucocratic, grayish-white granite, fine-grained, equigranular and isotropic, cropping out in elongated banks. Mineralogically, it is composed of abundant biotite (30%) dispersed and in nests, quartz and feldspar. Locally, slight deformation is observed in the granite. Petrographically, it is a medium- to coarse-grained, deformed granite with an interlobate equigranular texture. It is composed of feldspar (53-56%), quartz (35-38%), biotite (4-5%) and sericite-muscovite (1-8%). In some samples, garnet (<2%) occurs as a secondary mineral. The granites are cut by pegmatites dikes composed of quartz, feldspar, muscovite, biotite and green mica, and locally by basic rocks (gabbro or microgabbro) composed of abundant tabular plagioclase, pyroxene glomerulus and minor massive quartz (Gianotti & Arrighetti, 2017).

Piedra Los Indios Granite: Two textural types are distinguished: porphyroid and inequigranular. The porphyroid granite is the dominant lithology, cropping out in elongated boulders 7-12 m long. It is composed of alkali feldspar phenocrysts, white to pinkish-white in color, up to 10 cm long, showing a predominance of unidirectional magmatic orientation. The direction of the alkali feldspar lineation ranges from E–W±10° to N50, and the plane of magmatic foliation trends N68E to N70E. It also contains mafic minerals, abundant biotite and quartz, and is locally cut by microgabbro dikes. In other regions, the granite exhibits a medium- to coarse-grained matrix. The inequigranular granite occurs as well-defined boulders and domes. It is isotropic, composed of alkali feldspar (40-45%), quartz (25-30%), and biotite (25-35%). Biotite is highly abundant in the matrix, giving the rock a mesocratic character (Gianotti & Arrighetti, 2017).

Camacho Formation: Defined by Goso and Bossi (1966), it comprises a succession of sandstones ranging from very fine to coarse, siltstones and clayey pelites. It is notable for its abundant fossil content and attains a maximum thickness of approximately 15 m in outcrops (Perea & Martínez, 2009). A detailed stratigraphic column has been presented for the San Pedro locality, with an exposed thickness of 6 m, where light olive and light olive-grey pelitic deposits are identified, characterized by a high abundance of ichnofossils. These deposits are intercalated with tempestites, recognizable as very fine to fine sandstones of very light grey color, containing coquina arranged in strata or concretions, and various sedimentary structures, among which hummocky structures stand out (Sprechmann et al., 1994). The unit constitutes a shallow siliciclastic platform dominated by wave action. With variations in depth, the platform transitions to a progradational regime with gradual shallowing, which ultimately gives way upward to an estuarine regime with tidal influence and deltaic subenvironments (Ugalde, 2019). According to biostratigraphic and isotopic evidence provided by various researchers, the unit was deposited in the Late Miocene, approximately 10 Ma ago (Perea & Martínez, 2009).

Raigón Formation: Defined by Goso (1965), it is composed of fine- to very fine-grained, well-sorted sandstones with clay cement in varying proportions, massive, and light gray to ochre in color; medium- to coarse-grained sandstones, moderately to poorly sorted, subrounded to subangular, feldspathic, with variable clay content, yellowish-white to reddish in color; conglomeratic sandstones and polymictic conglomerates, subrounded to subangular, with minor clay content; lenses and beds of massive clays, green to greenish-gray in color, with variable sand fraction, up to clayey sandstones. The presence of calcareous concretions is common. This set is arranged in an interdigitated and broadly rhythmic manner, in lenticular beds with development of planar-parallel and cross-stratification, with an approximate thickness of 30 m. Deposition is suggested in a transitional and continental fluvial environment under semi-arid climate conditions (Preciozzi et al., 1985). Data reported by numerous researchers suggest an age ranging from the Late Pliocene to the Middle Pleistocene for the deposits of the Raigón Formation (Perea & Martínez, 2009).

Libertad Formation: Defined by Goso (1965), it is characterized by silty-clayey sediments containing fine-, medium-, and coarse-grained sand, gravel, and/or scattered pebbles, ranging in color from greenish-brown to red, lacking discernible stratification, and with thicknesses not exceeding 30 m. Carbonate occurs as powdery material, in concretions and/or thin beds. The sediments were likely deposited in a continental environment under arid conditions and associated with glacial episodes (Goso, 1965; Martínez & Ubilla, 2009). Various studies carried out in the south and east of Uruguay have provided multiple radiocarbon ages from different localities, ranging from 20 to 30 ka, which allow assigning the Libertad Formation an age corresponding to the Late Pleistocene (Ubilla & Martínez, 2016).

1.2 Hydrogeological Background

The study area comprises aquifers in rocks with fracture-induced porosity, exhibiting medium to high potential for groundwater. The Paleoproterozoic Hydrogeological Unit is developed in the southern and southwestern regions of the country and is composed of gneisses, granites, mica-schists and amphibolites. Specific discharge is approximately 1.0 m³/h/m, and the average dry residue reaches approximately 500 mg/L (Heinzen et al., 2003) (Figure 3).

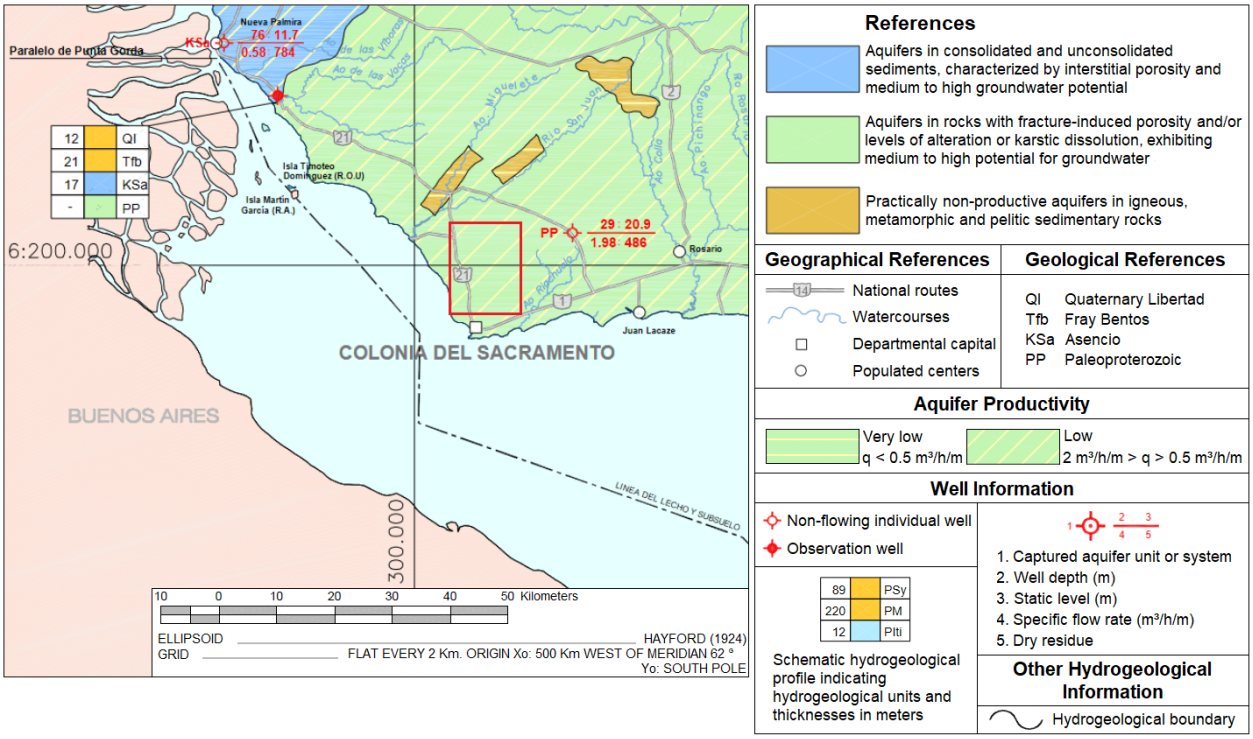

Figure 3. Section of the Hydrogeological Map of Uruguay at a scale of 1:1.000.000 (study area marked in red)

Source. Modified from Heinzen et al. (2003).

Fractured aquifer: In the study area, fractured aquifers are mainly composed of granites. The storage capacity of the Crystalline Basement aquifer unit is controlled by several factors, including the type and size of fractures, the interconnection of fractures, the rock type where fracturing occurs, and the fracture porosity, which is related to mechanical, chemical, and biological alteration processes (Montaño, 1999).

Generally, the Crystalline Basement exhibits alteration zones with thicknesses of less than five meters, with no possibility of significant storage. The storage capacity mainly depends on fracture porosity. Recharge originates from vertical transfer through the Libertad Formation when it overlies the basement, and from the contribution of streams and gullies channeled along fractures. Although the Libertad Formation exhibits very low permeability, its large areal extent allows the transfer of a significant volume to the fractured system (Montaño, 1999).

Hydraulic conductivities obtained in the laboratory through constant-head tests on sediments of the Libertad Formation range between 10^{-9} and 10^{-10} m/s, whereas field infiltration rates measured using double-ring infiltrometer tests show values between 10^{-7} and 10^{-8} m/s. This difference reflects the variability of soil structural conditions in the field, such as macropores or fissures, which are not captured in laboratory tests. Consequently, field infiltration rates are one hundred times higher than the hydraulic conductivities determined in the laboratory (Rodríguez et al., 2017).

Sedimentary aquifer: The Raigón Aquifer System is classified as a multilayer aquifer, which can range from unconfined to semi-confined, with the Camacho or Fray Bentos formations as the base and, when present, the Libertad or Dolores formations as the top (Postiglione et al., 2009).

In the locality of San Pedro, department of Colonia, vertical electrical soundings were conducted, allowing the identification of five layers. The first two layers are shallow and of no hydrogeological interest (Cicalese, 1998). The third layer exhibits an average resistivity of 32-33 Ω·m, with thicknesses ranging from 4 to 11 m and depths from 1.5 to 12 m; this layer is the one supplying water to the wells (Cicalese, 1998). The fourth layer exhibits very low resistivity of 5-6 Ω·m, occurs at depths between 7 and 44 m, and is characteristic of water with a high dissolved solids content (Cicalese, 1998). Below this layer, very high resistivities are recorded, indicating the presence of crystalline rocks with minimal or no potential for water circulation (Cicalese, 1998).

Furthermore, previous studies indicated that high electrical conductivity values were recorded in the study area, including several wells in the MEVIR settlement (Rural Housing Eradication Movement). These results, associated with sediments of the Camacho Formation, show that groundwater analysis reveals high chloride levels, likely due to the deposition of this geological formation in a marine-littoral environment (Goso Aguilar & Muzio, 2006).

2. Materials and Methods

A Solinst Model 101 probe was used to measure total well depth and water level. To analyze the hydrodynamic behavior of both aquifers, a survey of water points was conducted, encompassing a total of 32 wells. The inventory included data on location, total depth, water level, estimated flow rate, and well construction characteristics, which are essential for determining fracture depth, flow directions, and other parameters. A Hanna Instruments HI 9829 multiparameter probe was used to measure in situ physicochemical parameters, including electrical conductivity, pH, redox potential (Eh), dissolved oxygen, total dissolved solids, turbidity, and temperature. Groundwater samples were collected for major-ion analysis in 300-mL PET bottles, for arsenic and alkalinity analysis in sterile 50-mL Falcon tubes, and for bacteriological analysis in sterile 500-mL plastic bottles. Major-ion analyses were conducted at the Water and Soils Laboratory of the Centro Universitario Regional Litoral Norte (CENUR-LN, Litoral Norte Regional University Center), following established analytical methods (American Public Health Association [APHA] et al., 2017). Arsenic analyses were carried out at the Centro Especializado en Química Toxicológica (CEQUIMTOX, Specialized Center for Toxicological Chemistry) of the Faculty of Chemistry, using microwave-induced plasma atomic emission spectrometry coupled with hydride generation (HG-MIP OES, Agilent 4210) at λ = 193.695 nm. Alkalinity was determined in the field, following the corresponding technical standard (Menéndez, 2017). Bacteriological analyses were conducted at the Cooperativa Laboratorio Veterinario de Colonia (COLAVECO, Colonia Veterinary Laboratory Cooperative), determining total and fecal coliforms, *Pseudomonas aeruginosa,* and heterotrophic bacteria at 35 °C.

3. Results

3.1 Geology

Paleoproterozoic granites: Outcrops are restricted to small artisanal quarries in the eastern and southeastern parts of the study area. The granitic bodies exhibit meteoric alteration, low fracturing, and slight deformation (Figures 4A and F). In hand sample, the granite is leucocratic, grayish-white, with a holocrystalline, phaneritic, equigranular, hypidiomorphic, medium-grained texture. It is composed of quartz, plagioclase, biotite, and alkali feldspar (Figure 4D). In other areas of the quarry, the granite shows variation. In hand sample, it is leucocratic, grayish-white, with a holocrystalline, phaneritic, isotropic, inequigranular, hypidiomorphic, medium- to coarse-grained texture. Its main mineral constituents are quartz, biotite, plagioclase, and alkali feldspar (Figure 4E). The granitic body is cut by numerous dikes, mainly composed of quartz, with widths of up to 40 cm, which are in turn affected by faults trending NE-SW to E-W (Figures 4B and C).

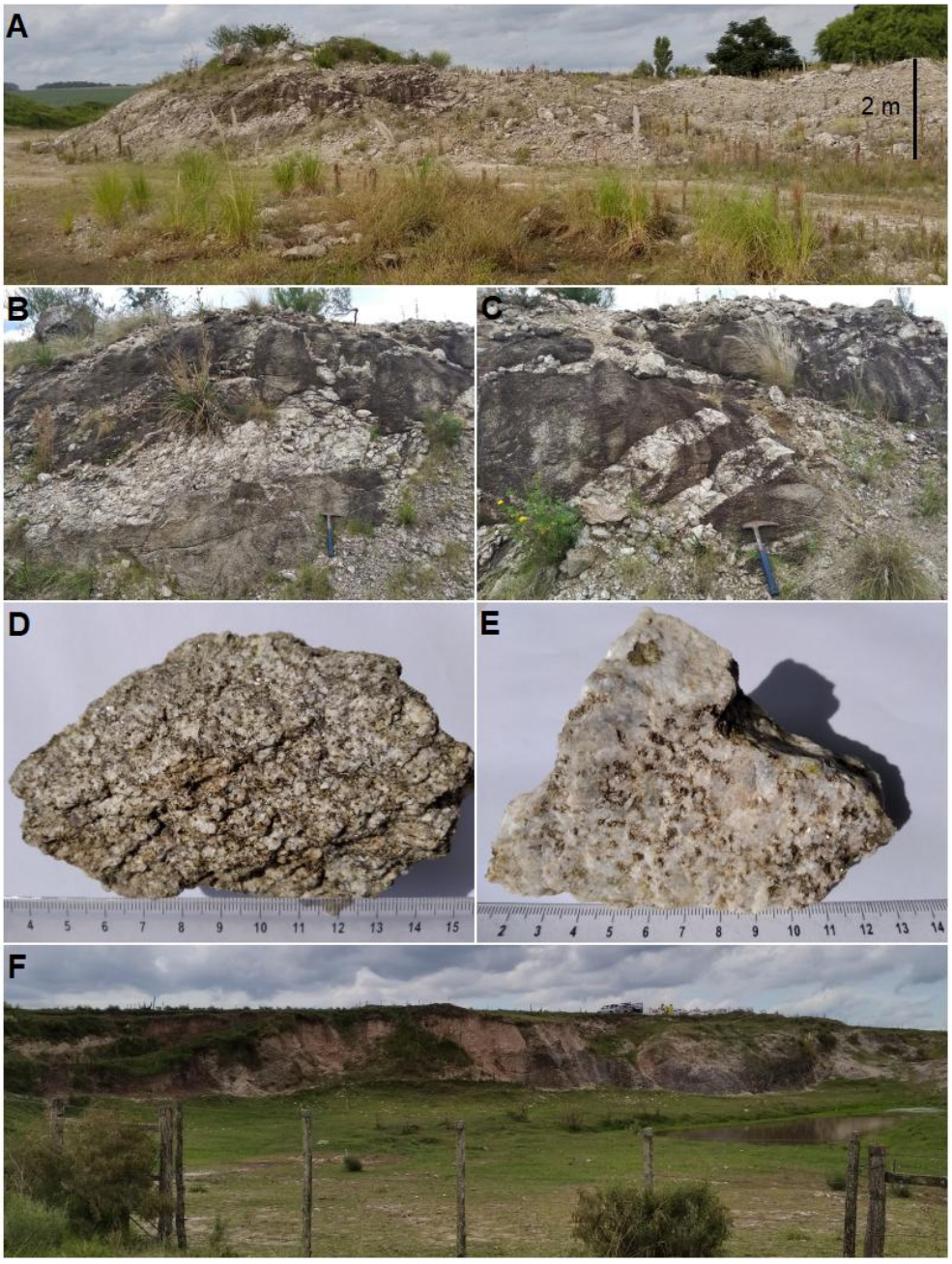

Figure 4. (A) General view of the outcrop in the southeastern sector of the study area. (B-C) Details of the outcrop cut by quartz dikes and affected by faults trending NE-SW to E-W. (D) Leucocratic, phaneritic, equigranular, hypidiomorphic, medium-grained granite, composed of quartz, plagioclase, biotite, and alkali feldspar. (E) Leucocratic, phaneritic, isotropic, inequigranular, hypidiomorphic granite, medium- to coarse-grained, mainly composed of quartz, biotite, plagioclase, and alkali feldspar. (F) General view of the outcrop in the eastern sector of the study area

Camacho Formation: The unit is well exposed in the cliffs at the Brisas del Plata locality, located in the western part of the study area (Figures 5A and B). This formation consists of light-gray, consolidated siltstones, containing white, spherical to oval concretions up to 30 cm in length, bivalve impressions up to 4 cm, and *Thalassinoides* burrows (Figures 5C and D). These deposits are interbedded with very fine-grained, 20-50 cm-thick tempestite sandstones (Ugalde, 2019). The unit has an exposed thickness of up to 7 m.

Raigón Formation: The unit is recognized in the cliffs at the Brisas del Plata locality, overlying the Camacho Formation at an erosional contact. Sandstones of variable grain size, ranging from fine to very coarse, containing scattered granule-sized clasts, light brown in color, poorly consolidated, and moderately to poorly sorted. They exhibit a clast-supported texture, with grains predominantly subangular to subrounded. The composition is predominantly quartz-feldspar, with lithic fragments (Figure 5E). The formation reaches a thickness of up to 4 m in outcrops and occurs interdigitated, with sequences of medium- to coarse-grained levels.



Figure 5. (A-B) General view of the cliffs at Brisas del Plata (camping site). (C) Detail of light-gray siltstones with spherical to oval calcareous concretions, interbedded with thin levels of very fine sandstones (Camacho Formation). (D) Hand sample of light-gray siltstone with bivalve impressions (Camacho Formation). (E) Hand sample of sandstone with variable grain size, light brown in color, poorly consolidated, moderately to poorly sorted, with a clast-supported texture and a quartz-feldspar composition, containing lithic fragments (Raigón Formation)

3.2 Hydrogeology

Two aquifer units were identified in the study area, one composed of granites belonging to the Crystalline Basement, forming a fractured aquifer, and another composed of the Raigón Formation, forming a sedimentary aquifer. Based on its lithological characteristics, the Libertad Formation behaves as an aquiclude, whereas in the Carrasco Creek Basin (department of Montevideo) it would function as an aquitard (Montaño, 1999). In the study area, the Libertad Formation covers 40% of both aquifers, providing natural protection against potential contaminants. The inventoried wells were identified by an abbreviation and a number (Figure 6).

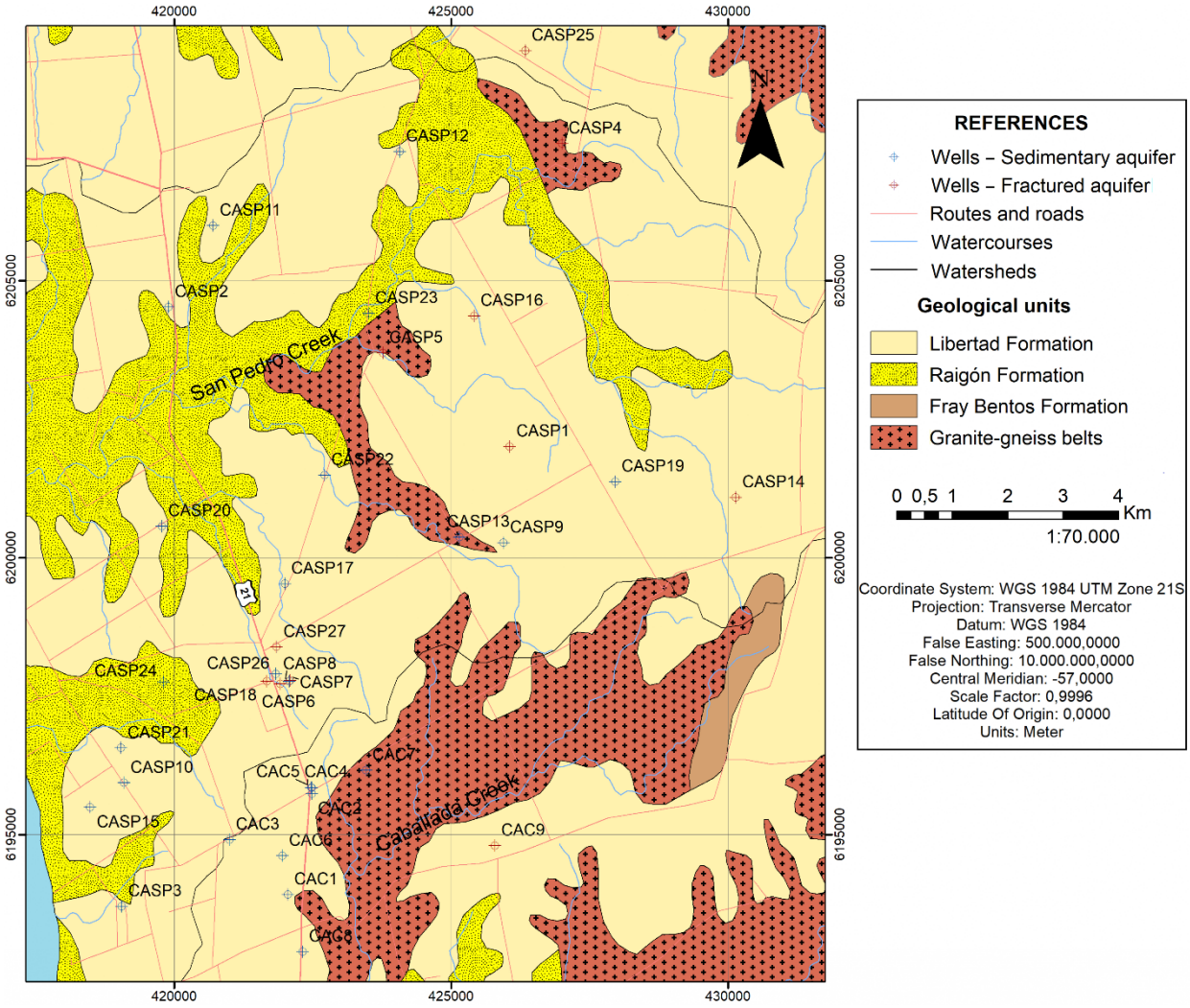

Figure 6. Well locations in the study area

3.2.1 Fractured aquifer

The granites of the Crystalline Basement constitute a fractured aquifer that extends across the entire study area. It crops out to the east, covering approximately 30% of the surface, and behaves as an unconfined aquifer. To the north and west, it is covered by the Raigón Formation over 30% of the area and the Libertad Formation over 40%, behaving as a confined to semi-confined aquifer. The main fracture orientations are NE-SW. Groundwater from this aquifer is primarily used for human consumption in rural schools, the MEVIR settlement, and dairy farms. Based on the well inventory (see Table S1 in the Supplementary Material), the total well depth, fracture depth, water level, and estimated flow rate were analyzed. The results of this analysis are presented below.

Total well depth (m): An average depth of 35.25 m was obtained, with a maximum of 48 m at well CASP4 and a minimum of 20 m at well CASP6. Data analysis indicates that the water-bearing fractures are located at depths between 20 m and 48 m (Figure 7).

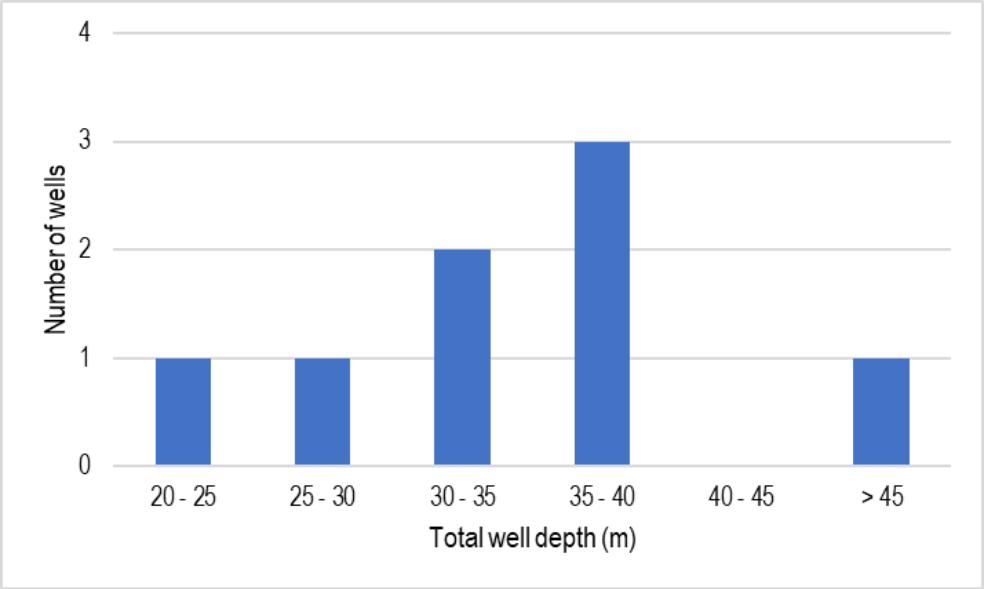

Figure 7. Frequency of total well depth (m) in the fractured aquifer (n = 8)

Flow rate (m^3/h): The flow rate data correspond to the values provided by the well owners, reflecting the operational flow. No well efficiency tests, which are the standard methodology for estimating optimal flow rate, were conducted in this study. It should be noted that flow rate depends on the structural condition of the wells. In fully cased wells, it is also influenced by the pump installation depth, the length of the water delivery pipe, and the pump's power and control settings. Based on the flow rate data provided, an average value of 7.55 m^3/h was obtained, with a maximum of 12 m^3/h in wells CASP1 and CASP18, and a minimum of 3 m^3/h in well CASP25 (Figure 8).

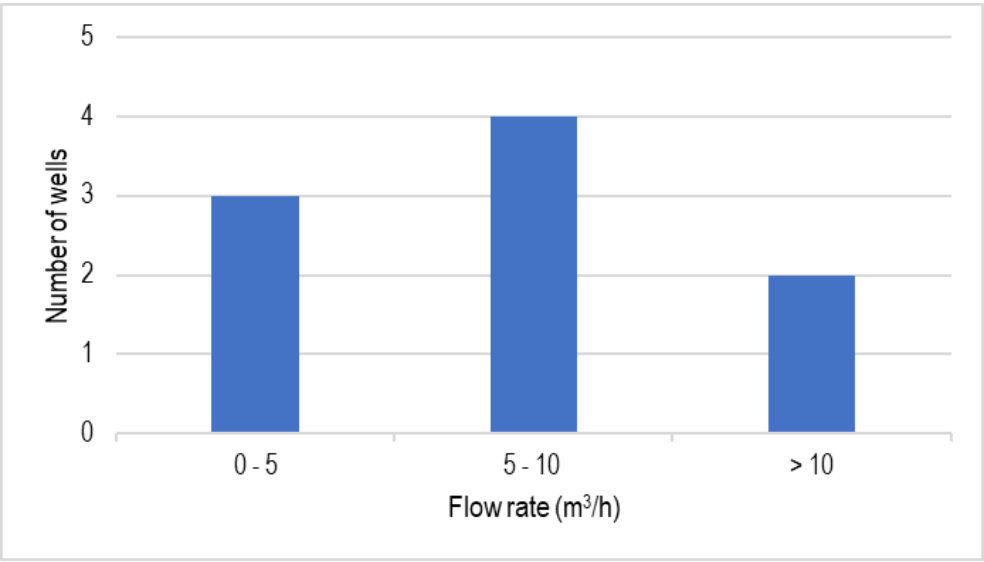

Figure 8. Frequency of flow rate (m^3/h) in the fractured aquifer (n = 9)

To evaluate possible trends or relationships between flow rate and total well depth, a graph was plotted using these values. A slight tendency for flow rate to increase with depth was observed (Figure 9). Furthermore, it is evident that wells with the same total depth of 40 m exhibit highly variable flow rates, which supports the concept of the hydraulic conductor (Montaño, 1999), according to which fracturing is a localized phenomenon.

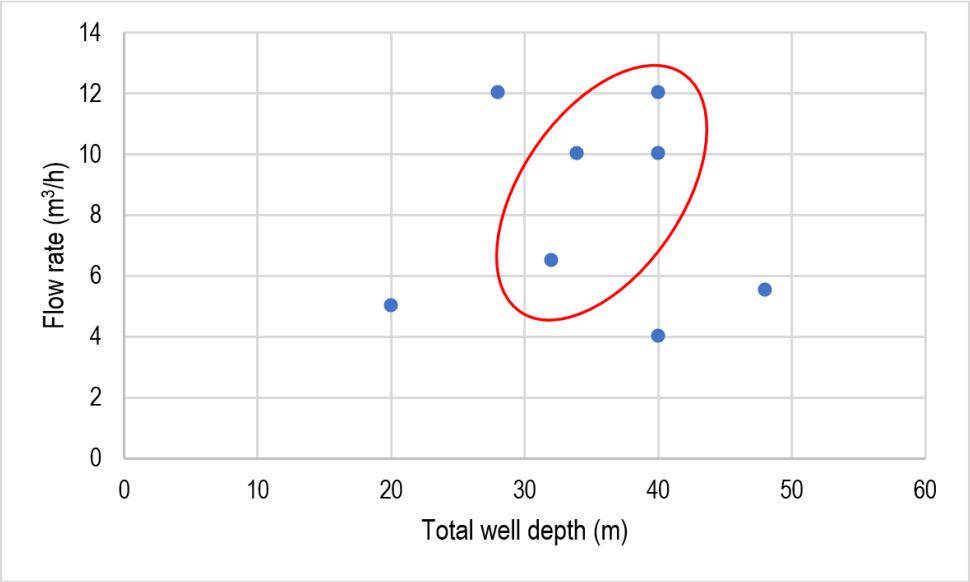

Figure 9. Flow rate vs. total well depth in the fractured aquifer

Static level (m): The analysis indicates that the average static level was 6.79 m, with a maximum of 19.17 m at well CASP4 and a minimum of 0.78 m at well CASP5 (Figure 10). This information, together with ground elevation, is essential for developing the piezometric map of the studied aquifer.

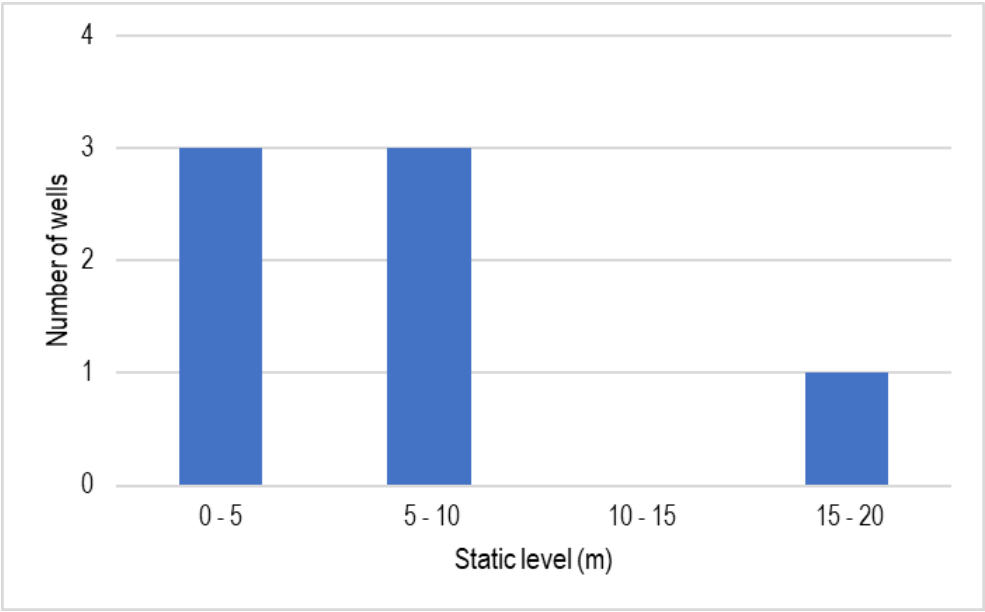

Figure 10. Frequency of static level (m) in the fractured aquifer (n = 7)

Piezometry: The piezometric map of the fractured aquifer for May 2021 shows a predominant groundwater flow in the southeast-northwest direction (Figure 11). In general, the piezometric surface is relatively flat; however, in the central-east sector, a slight radial divergence is observed between wells CASP16 and CASP1, with hydraulic gradients of 0.004 (i_2) and 0.005 (i_4), suggesting a recharge area. Hydraulic gradients are higher in the central-west sector, with values of 0.005 (i_3) and 0.007 (i_1), and in the southwest sector, with a value of 0.009 (i_8), which may indicate natural discharge zones of the aquifer. In the central-south sector, hydraulic gradients are relatively uniform, with values of 0.0051 (i_7), 0.0052 (i_6), and 0.0055 (i_5).

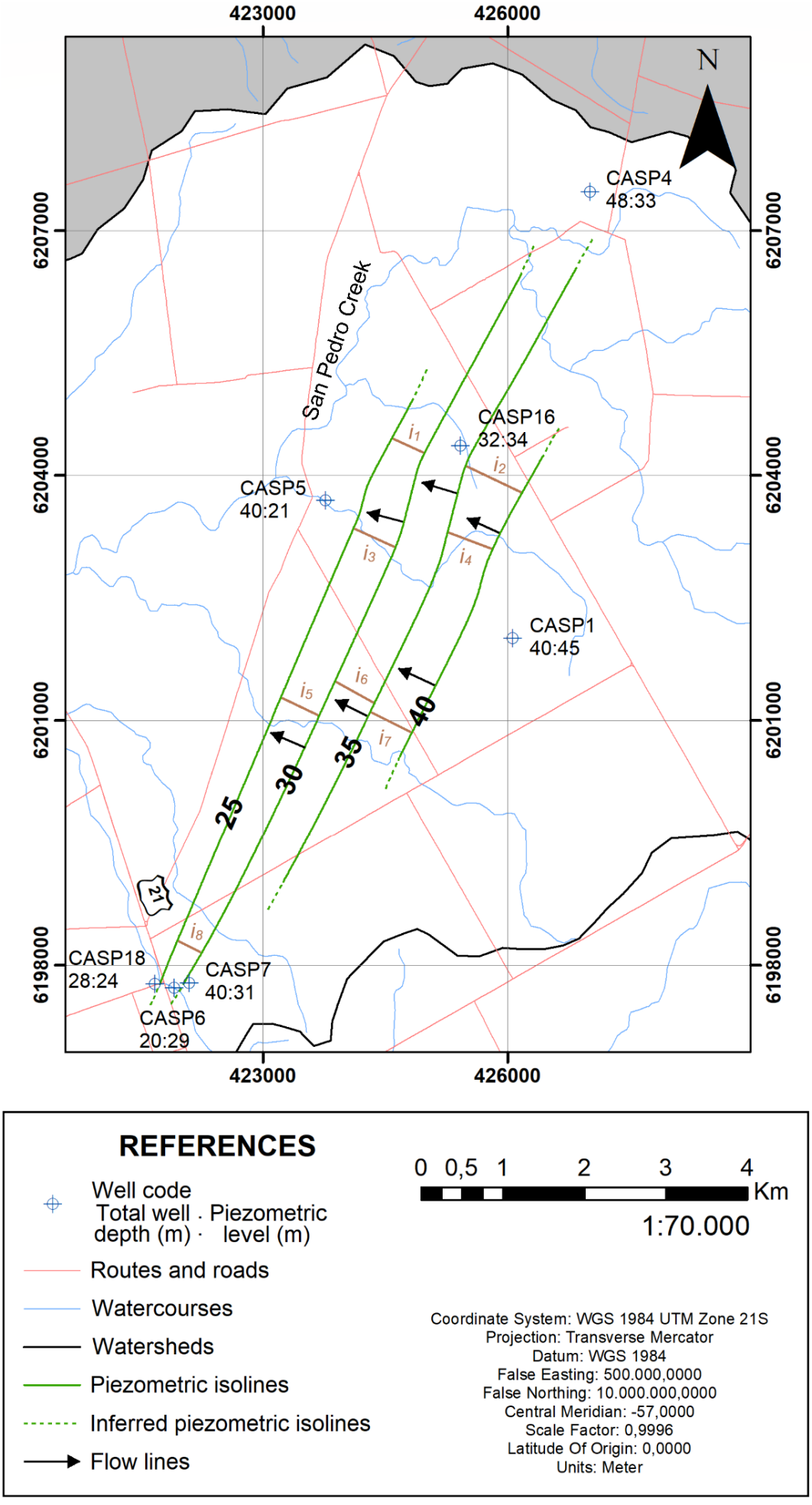

Figure 11. Fractured aquifer piezometric map. San Pedro, Colonia. May 2021

3.2.2 Sedimentary Aquifer

The Raigón Formation constitutes the main sedimentary aquifer, with widespread distribution throughout the study area. It is composed of permeable sandstone layers interbedded with clay levels. The thickness of the unit varies across the study area, averaging approximately 10 m and pinching out to the northwest, while overlying the granites of the Crystalline Basement. It exhibits unconfined aquifer behavior in its outcropping portion along the coast and at the margins of the San Pedro Creek, with elevations up to 60 m above sea level. It behaves as a semi-confined aquifer when overlain by the Libertad Formation, covering approximately 40% of its surface extent.

Based on the well inventory (see Table S2 in the Supplementary Material), the total well depth, static water level, and estimated flow rates were analyzed. A total of 25 wells were inventoried, of which 13 are walled wells, and 12 are semi-artesian wells. Walled wells are mainly distributed in the southern sector of the study area, generally at the highest elevations, reaching up to 61 m above sea level. In these zones, the sediment thickness is greater, and the wells are primarily used for domestic purposes and, secondarily, for dairy farming. Most of them are located close to dwellings, at a distance of less than 10 m. On the other hand, semi-artesian wells are mainly located in the southwestern sector, at elevations ranging from 17 to 60 m above sea level. They are used for domestic purposes and dairy farming. Most of them are situated close to dwellings (less than 10 m), although some are more than 30 m away, and others are near dairy facilities or livestock. The following section provides a detailed analysis of each type of well construction.

Walled wells: The analysis indicates that the average total well depth was 13.03 m, with a maximum of 27.36 m at well CAC1 and a minimum of 3.9 m at well CAC8, both located in the southern part of the study area. In general, the deepest wells were found in higher topographic zones. With respect to flow rate, only two data points provided by the owners were available, with values of 0.7 m^3/h at well CASP9 and 2 m^3/h at well CASP3, located in the eastern and western sectors of the region, respectively. The average static water level was 9.35 m, with a maximum of 19.77 m at well CAC1 and a minimum of 1.69 m at well CAC8, both situated in the southern part of the study area.

Semi-artesian wells: The data analysis shows that total well depth averages 27 m, with a maximum of 37 m at well CASP19 and a minimum of 15 m at well CASP21, located in the eastern and western parts of the study area, respectively (Figure 12).

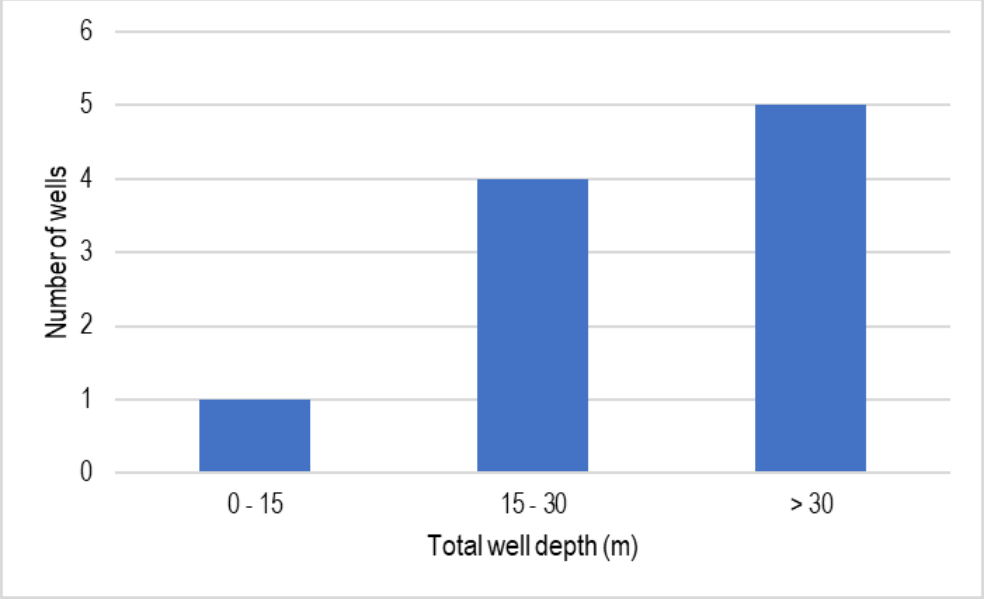

Figure 12. Frequency of total well depth (m) in semi-artesian wells of the sedimentary aquifer (n = 10)

With respect to flow rate, based on owner-provided data, the average flow rate was 3.65 m^3/h, with a maximum of 6 m^3/h at well CASP20 and a minimum of 1.8 m^3/h at well CAC4 (Figure 13).

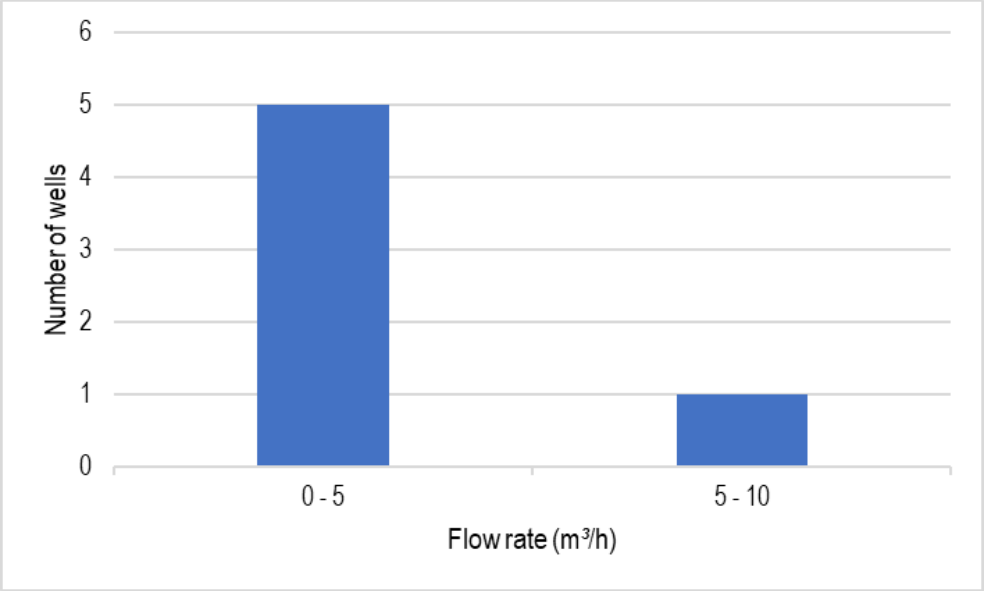

Figure 13. Frequency of flow rate (m^3/h) in semi-artesian wells of the sedimentary aquifer (n = 6)

Based on total well depths and owner-reported flow rates, a graph was constructed to evaluate possible trends or relationships between the two variables (Figure 14). The analysis shows a general trend of increasing flow rate with depth, although some wells exhibit similar flow rates despite differing depths.

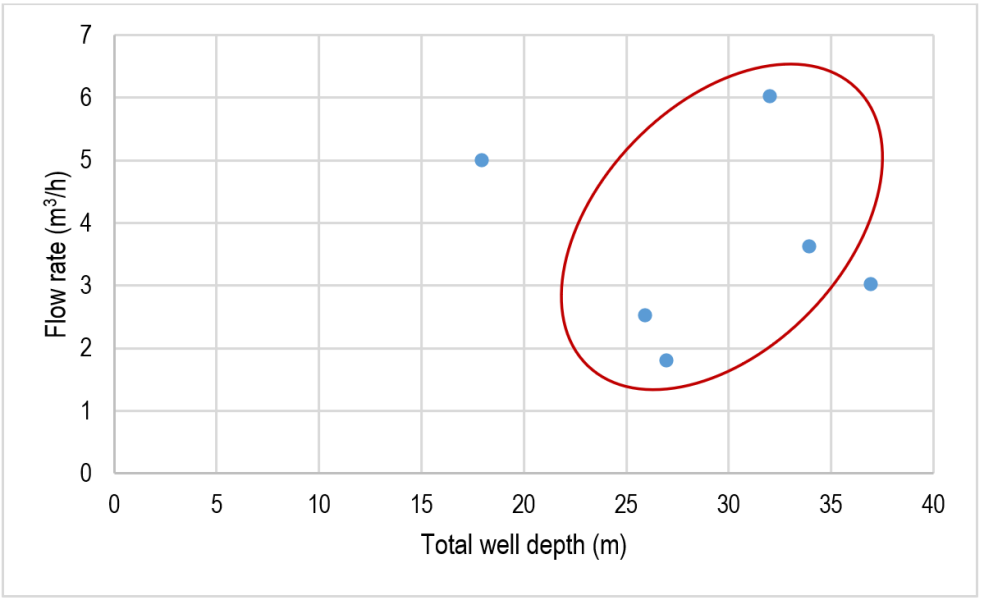

Figure 14. Flow rate vs. total well depth in the sedimentary aquifer

Analysis of static water level data indicates that the average value was 7.24 m, with a maximum of 9.5 m at well CASP15 and a minimum of 2.64 m at well CASP22, located in the southwestern and northern parts of the study area, respectively (Figure 15). This information, together with ground elevation data, is essential for constructing the piezometric map of the studied aquifer.

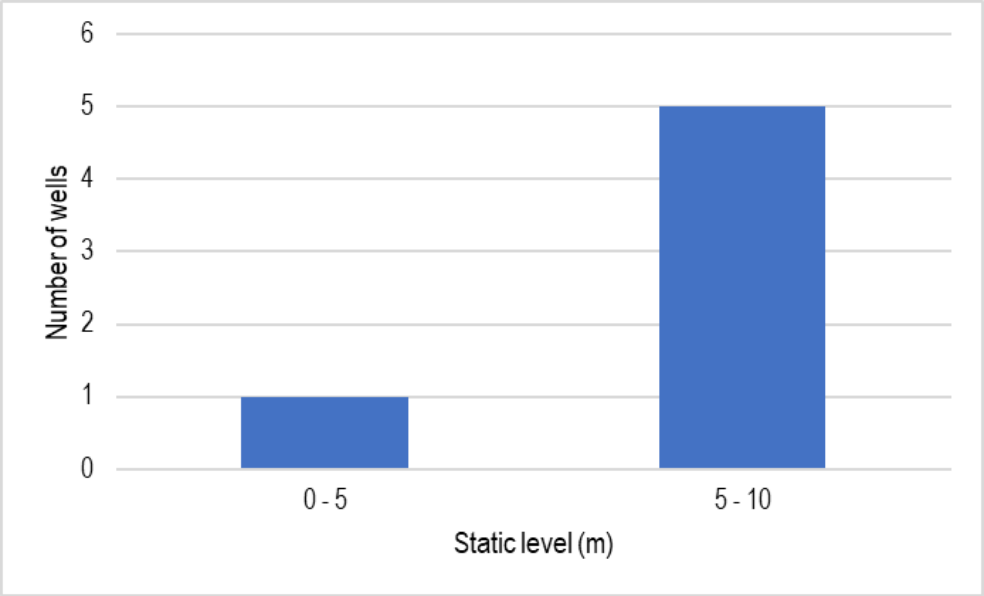

Figure 15. Frequency of static level (m) in the sedimentary aquifer (n = 6)

The piezometric map of the sedimentary aquifer for May 2021 shows groundwater flow generally directed south-east-northwest in the northern sector and northeast-southwest in the southern sector (Figure 16). In the western sector, the piezometric surface exhibits a convergent radial pattern at its northeastern end and a divergent radial pattern at its southeastern end. In this sector, near well CASP20, with a piezometric head of 12 m, hydraulic gradients of 0.003 (i_1) and 0.005 (i_5) were observed, suggesting a discharge area with flow directed westward toward San Pedro Creek. In the eastern sector, the piezometric surface exhibits a convergent radial pattern; near well CASP19, with a piezometric head of 52 m, a hydraulic gradient of 0.004 (i_4) was recorded, suggesting a recharge area for this sector. In the central sector, between these two areas, hydraulic gradients of 0.007 (i_3) and 0.008 (i_2) were identified in the northern zone, values of 0.006 (i_6) and 0.007 (i_7) in the central zone, and higher gradients in the southern zone, 0.013 (i_8) and 0.020 (i_9), indicating a discharge area in the latter case.

3.3 Hydrochemistry and Water Quality

Groundwater chemical characterization was carried out by collecting 33 samples, of which 23 correspond to wells extracting water from the sedimentary aquifer and 10 from the fractured aquifer. The results of the chemical analyses were evaluated based on the ionic balance by applying the error calculation equation (APHA, 1998). All samples were considered satisfactory.

3.3.1 Fractured Aquifer

The analysis of physicochemical parameters indicates that, in general, the groundwater complied with the limits established for drinking water according to UNIT 833:2008 (Instituto Uruguayo de Normas Técnicas [UNIT], 2008). However, two samples (wells CASP27 and CAC9) exhibited turbidity above the maximum permissible value. The results of the measured physicochemical parameters are presented below and summarized in Table 1, which reports the mean, maximum, and minimum values for groundwater from the fractured aquifer. The full dataset, including all parameters measured for each well, is provided in Supplementary Table S3.

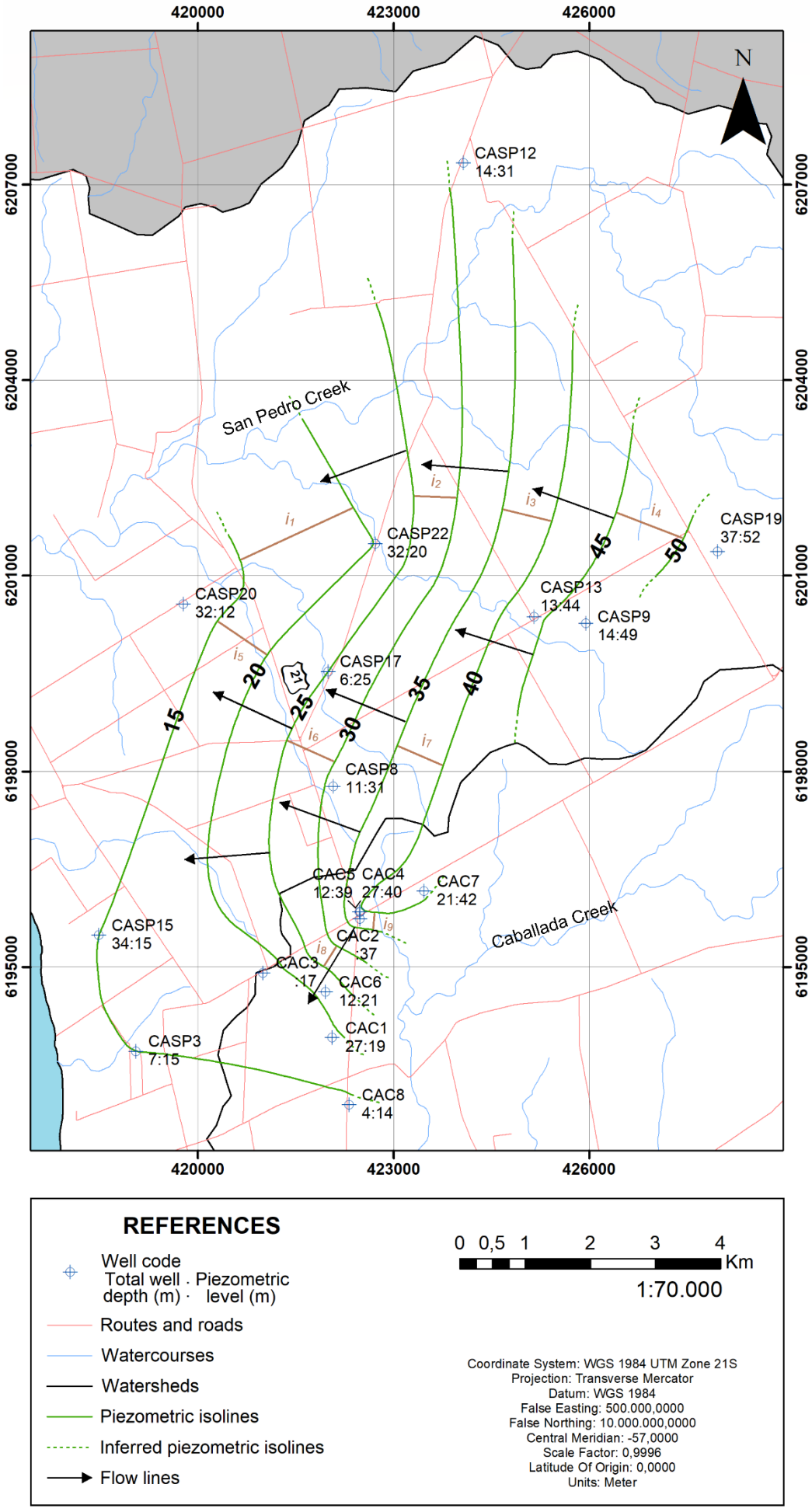

Figure 16. Sedimentary aquifer piezometric map. San Pedro, Colonia. May 2021

Table 1. Mean, maximum, and minimum values of the physicochemical parameters measured in groundwater from the fractured aquifer

Physicochemical Parameter	Mean Value	Maximum Value (Well)	Minimum Value (Well)
Electrical Conductivity (µS/cm)	936	1365 (CASP27)	691 (CASP14)
pH	7.2	7.4 (CASP4)	6.91 (CASP5)
Redox Potential (Eh) (mV)	191.92	224.6 (CASP14)	140.3 (CASP27)
Dissolved Oxygen (ppm)	4.2	6.5 (CASP25)	2.71 (CASP27)
Total Dissolved Solids (ppm)	468.5	685 (CASP27)	346 (CASP14)
Turbidity (FNU)	0.27	1 (CASP6)	0 (CASP16. CASP18)
Temperature (°C)	17.02	19.03 (CASP5)	14.18 (CAC9)
Total Hardness (mg $CaCO_3$/L)	272.72	346.8 (CASP25)	153.5 (CASP4)

Note. The maximum turbidity values (1.4 and 1.6 FNU in wells CASP27 and CAC9) were excluded from the analysis, as they exceed the maximum limit allowed for drinking water.

Electrical Conductivity: Elevated values were identified in the southern and west-southwestern sectors, likely associated with sediments of the Camacho Formation, whereas lower values predominated in the central-northern and eastern sectors. No clear relationship was observed between electrical conductivity and the direction of groundwater flow. All samples were below the maximum permissible limit for drinking water established by UNIT 833:2008 (Figure 17).

pH: Higher values were generally recorded in the eastern half, particularly in areas of greater topographic elevation, while lower values occurred in the western half. The pH range (6.91-7.4) corresponded to neutral conditions. A trend of increasing pH with higher nitrate concentrations, together with a decrease in pH along the groundwater flow direction, was observed. All samples complied with the drinking-water quality range established by UNIT 833:2008 (Figure 18).

Redox Potential (Eh): The greatest Eh values were recorded in the central-northern and eastern sectors, whereas the lowest occurred in the southern and west-southwestern sectors. The Eh values also varied slightly but remained positive. No consistent pattern with groundwater flow direction was observed.

Dissolved Oxygen: Higher concentrations were observed in the central-northern and eastern sectors, whereas lower concentrations were recorded in the southern and southwestern sectors. A decrease in dissolved oxygen concentration was observed in the direction of groundwater flow.

Total Dissolved Solids (TDS): The highest TDS values were distributed in the southern and west-southwestern sectors, whereas lower values were generally observed in the central-northern and eastern sectors, consistent with the relationship between electrical conductivity and TDS. No apparent relationship with the direction of groundwater flow was observed. All samples were below the maximum permissible limit for drinking water established by UNIT 833:2008 (Figure 19).

Turbidity: Higher turbidity was observed in the southern and west-southwestern sectors, whereas lower values were generally found in the central-northern and eastern sectors. No apparent relationship was found between groundwater flow direction and turbidity. With the exception of wells CASP27 and CAC9, all samples complied with the maximum permissible limit for drinking water established by UNIT 833:2008.

Temperature: Higher temperatures were recorded in the central-western and southwestern sectors, while lower temperatures were generally observed in the north-northeastern and southern sectors. No apparent relationship with groundwater flow direction was observed. All samples exhibited temperatures within the normal range for groundwater.

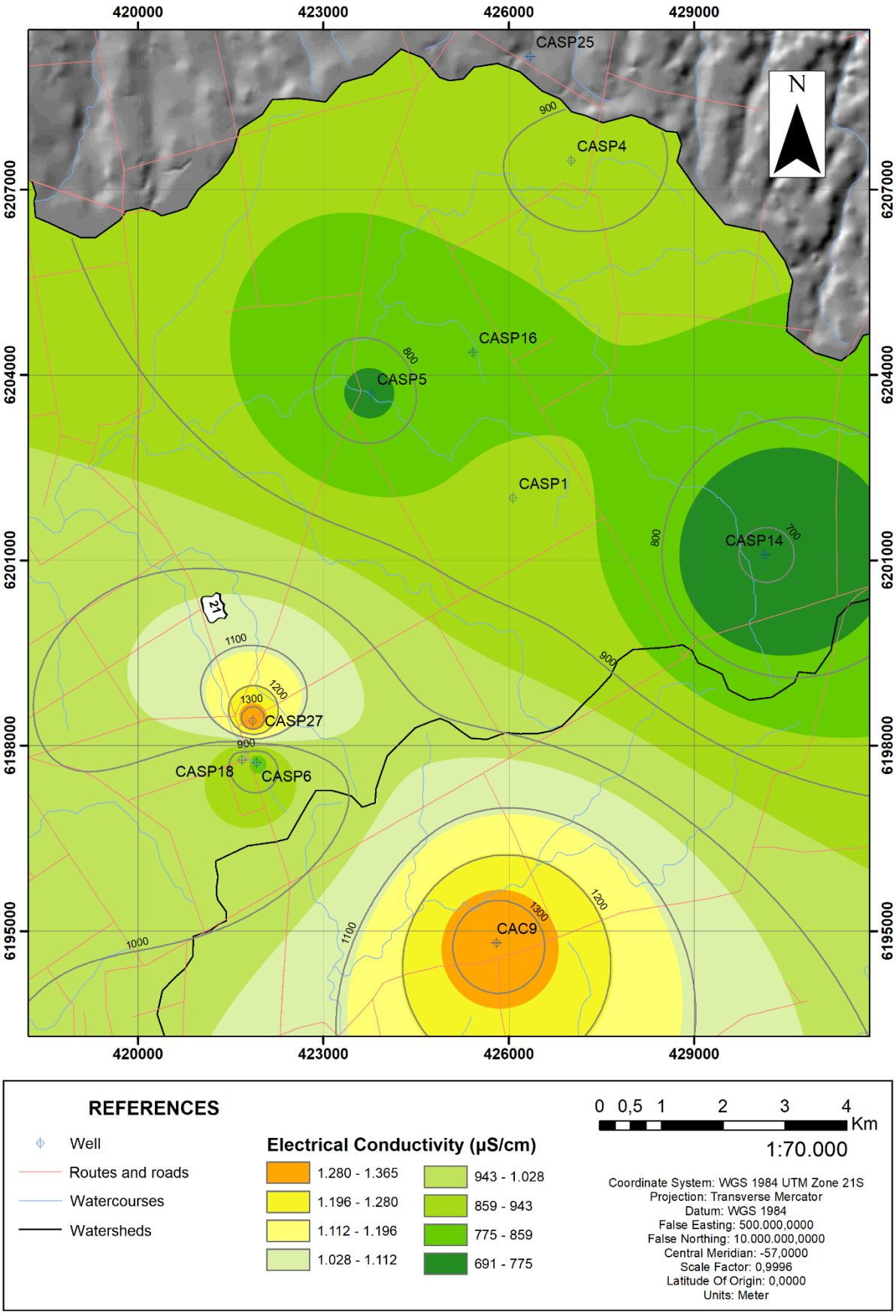

Figure 17. Fractured aquifer electrical conductivity map (µS/cm), San Pedro, Colonia

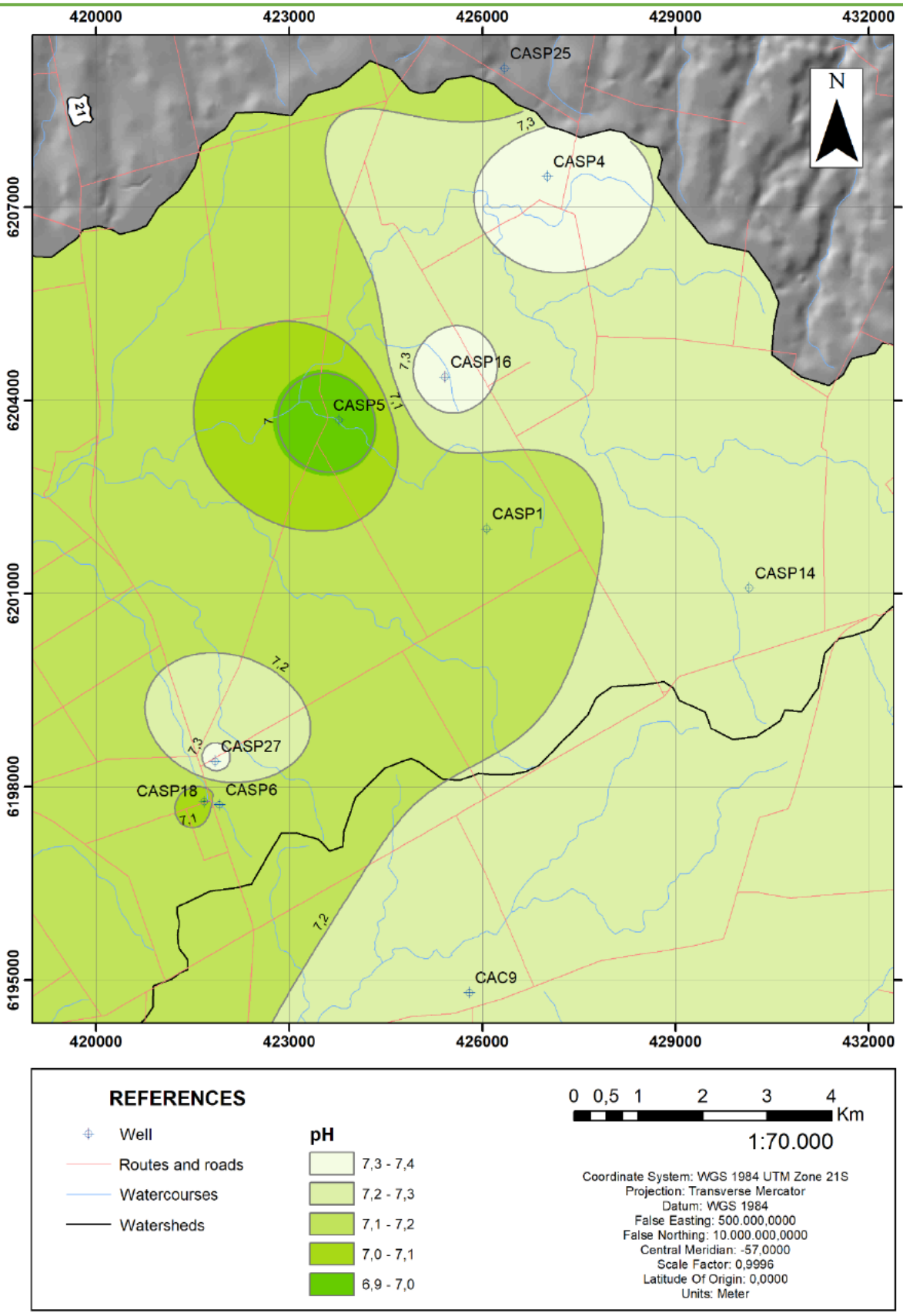

Figure 18. Fractured aquifer pH map, San Pedro, Colonia

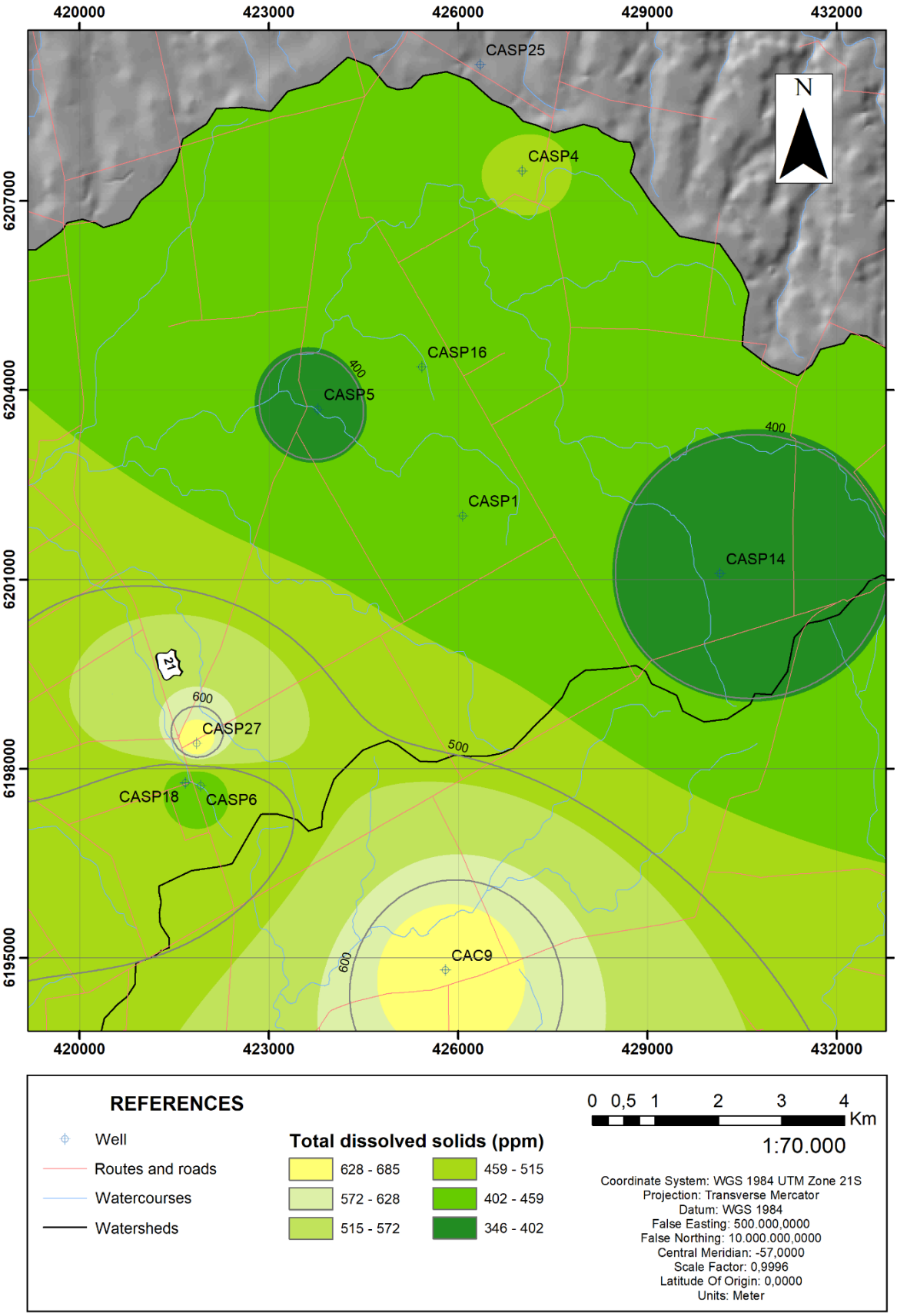

Figure 19. Fractured aquifer total dissolved solids map (ppm), San Pedro, Colonia

Total Hardness: Elevated hardness was generally located in the central-south and northern sectors, whereas lower values occurred in the north-northeast sector. No apparent relationship was found between groundwater flow direction and total hardness. Based on the mean total hardness, the water was classified as very hard. All samples were below the maximum permissible limit for drinking water established by UNIT 833:2008.

Based on the results of the chemical analyses, it was observed that, in general, the groundwater complied with the limits established for drinking water according to UNIT 833:2008 (UNIT, 2008), although some exceptions were noted. Nitrate concentrations in well CASP25 and total arsenic in well CASP4 exceeded the maximum values allowed by the standard, whereas, for total arsenic, only the sample from well CASP5 fell below the value recommended by the World Health Organization (WHO, 2021). The results of the chemical analyses are summarized in Table 2, showing the mean, maximum, and minimum concentrations of groundwater from the fractured aquifer. The full dataset, including all chemical parameters determined for each well, is provided in Supplementary Table S5.

Table 2. Mean, maximum, and minimum concentrations of chemical analyses in groundwater from the fractured aquifer

Chemical Element	Mean Concentration (mg/L)	Maximum Value (Well) (mg/L)	Minimum Value (Well) (mg/L)
Chlorides (Cl^-)	26.81	122.36 (CAC9)	3.04 (CASP27)
Nitrates (NO_3^-)	19.27	44.54 (CASP4)	0.08 (CASP14)
Bicarbonate (HCO_3^-)	486.66	545.34 (CASP14)	314.76 (CASP27)
Sulfates (SO_4^{2-})	13.11	23.19 (CASP4)	4.55 (CASP27)
Total arsenic (As)	0.017	0.034 (CASP4)	0.009 (CASP5)
Sodium (Na^+)	33.19	87.53 (CAC9)	3.57 (CASP27)
Potassium (K^+)	3.87	13.02 (CASP5)	0.29 (CAC9)
Magnesium (Mg^{2+})	5.17	9.46 (CASP5)	0.53 (CAC9)
Calcium (Ca^{2+})	19.35	80.47 (CASP7)	1.61 (CASP16)

Note. The maximum nitrate concentration (56.64 mg/L in well CASP25) was excluded from the analysis, as it exceeds the maximum limit allowed for drinking water.

Chlorides (Cl^-): The highest concentration was observed in the southern sector, whereas the lowest value was observed in the southwest. No apparent relationship was found between groundwater flow direction and chloride concentrations. All samples were below the maximum limit allowed for drinking water according to UNIT 833:2008.

Nitrates (NO_3^-): Elevated concentrations were observed in the northern sector, while the lowest were recorded in the southern and eastern sectors, likely associated with confined aquifer conditions. No relationship was observed between groundwater flow direction and nitrate concentrations. All samples, except for well CASP25, were below the maximum limit allowed for drinking water according to UNIT 833:2008 (Figure 20).

Bicarbonate (HCO_3^-): Higher concentrations were observed in the eastern half of the study area, whereas lower values occurred in the western half. A decrease in bicarbonate concentration along the groundwater flow direction was observed. According to UNIT 833:2008, no maximum limit is established for this parameter.

Sulfates (SO_4^{2-}): The greatest concentration was recorded in the north-northeast sector, while the lowest value was observed in the southwest. No relationship was observed between groundwater flow direction and sulfate concentrations. All samples were below the maximum limit allowed for drinking water according to UNIT 833:2008.

Total Arsenic (As): Elevated total arsenic concentrations may be attributed to both natural processes and anthropogenic influences. An increasing trend in arsenic concentrations with rising nitrate levels was observed, suggesting an impact from agricultural activities. The anomalous concentration was recorded in the north-

northeast sector, while the lowest was observed in the central-west sector. No relationship with groundwater flow direction was identified. Only the sample from well CASP4 exceeded the maximum limit established by UNIT 833:2008, and only the sample from well CASP5 was below the value recommended by the WHO (2021) (Figure 21).

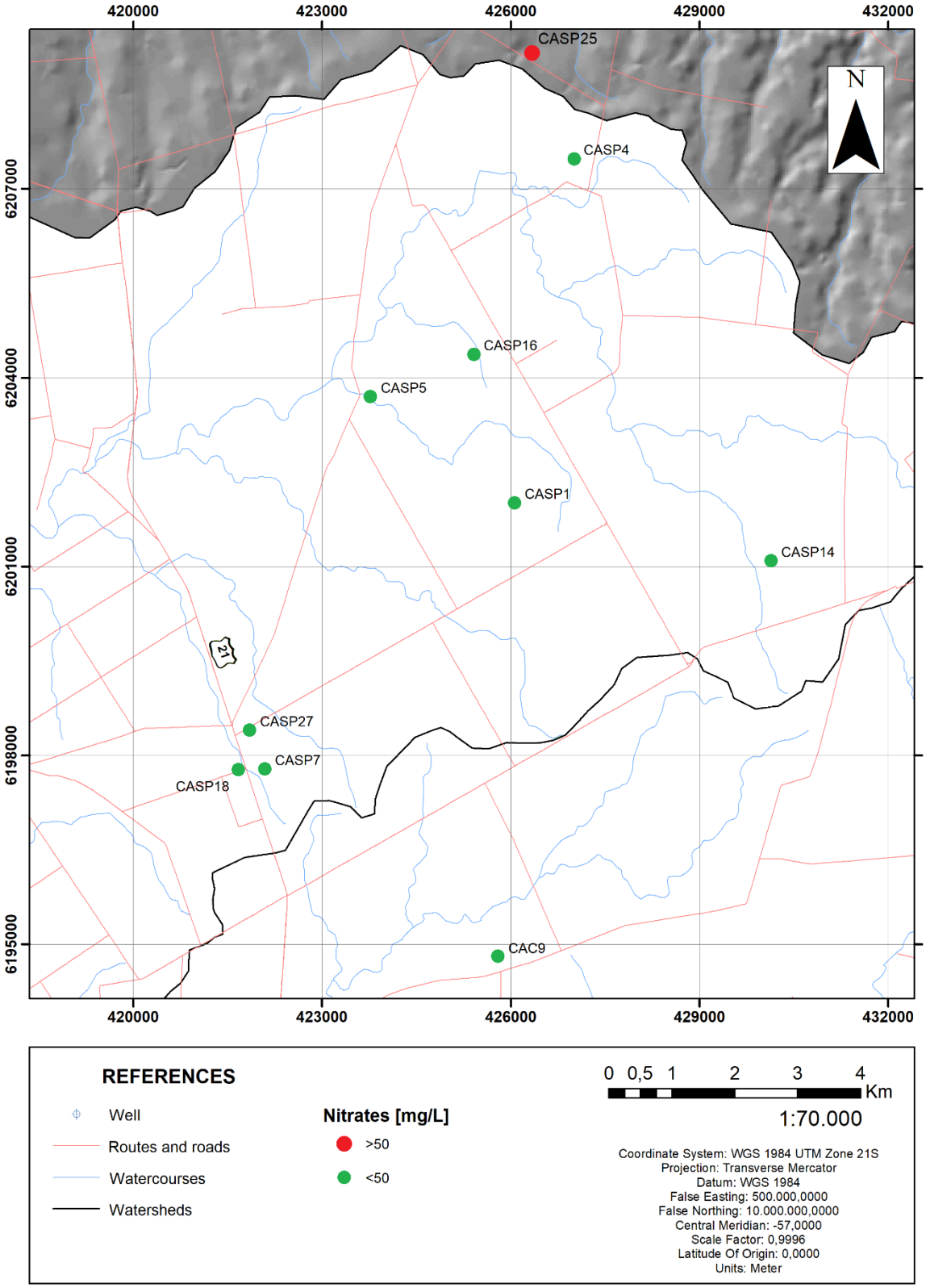

Figure 20. Fractured aquifer groundwater nitrates concentration map [mg/L], San Pedro, Colonia

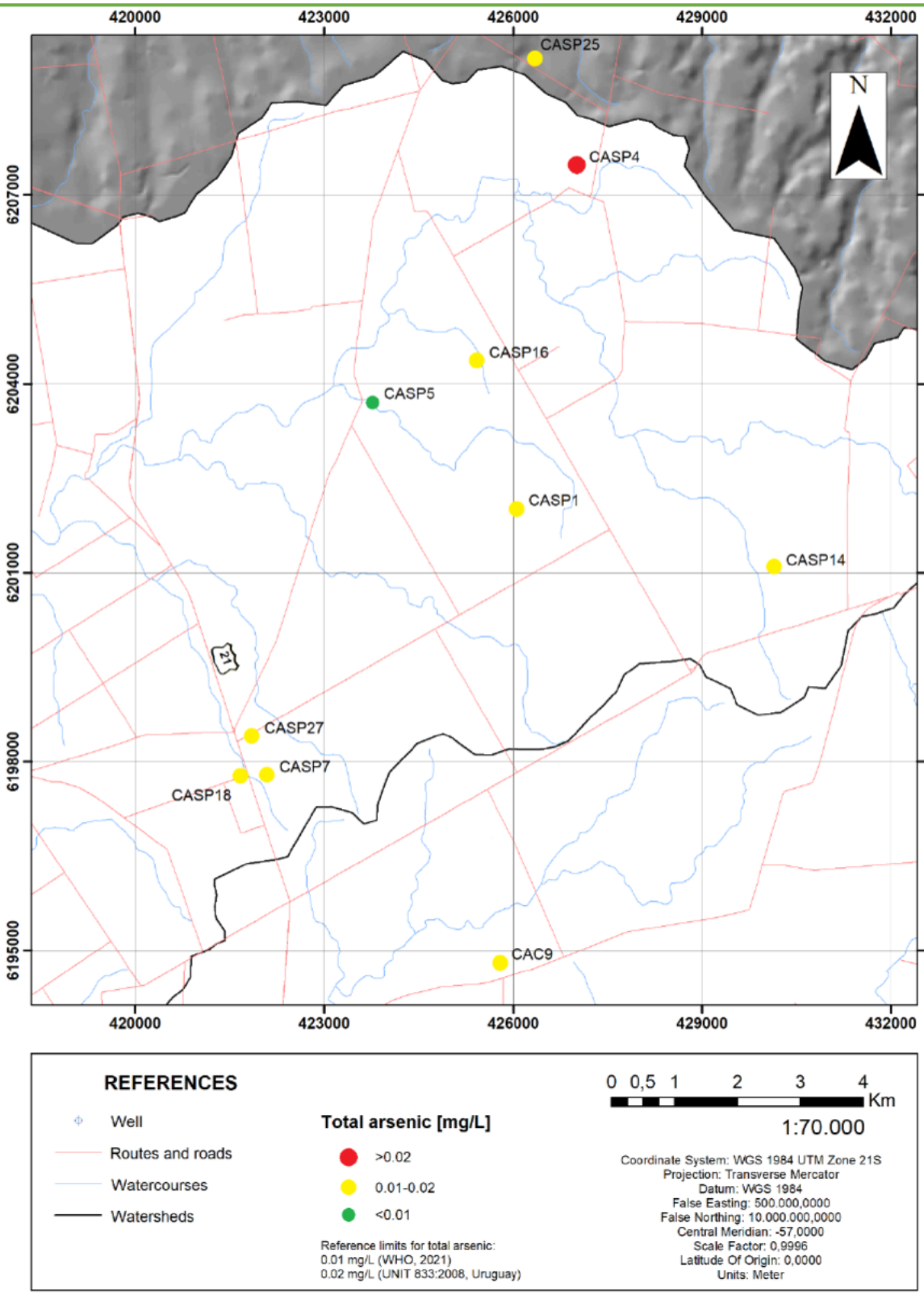

Figure 21. Fractured aquifer groundwater total arsenic concentration map [mg/L], San Pedro, Colonia

Sodium (Na^+): The highest concentrations were recorded in the north-northeastern and southern sectors, whereas lower values occurred in the central-western and southwestern sectors. A decrease in sodium concentration along the groundwater flow direction was observed. All samples were below the maximum limit allowed for drinking water according to UNIT 833:2008.

Potassium (K^+): Anomalous concentrations were observed in the central-northern and central-western sectors, while lower value was recorded in the southern sector. No relationship was observed between groundwater flow direction and potassium concentrations. UNIT 833:2008 does not establish a maximum limit for this parameter.

Magnesium (Mg^{2+}): The greatest concentrations were observed in the central-northern and central-western sectors, whereas lower values occurred in the southern and southwestern sectors. No relationship was observed between groundwater flow direction and magnesium concentrations. According to UNIT 833:2008, no maximum limit is established for this parameter.

Calcium (Ca^{2+}): Higher concentrations were found in the southwestern and northern sectors, while lower values were recorded in the central-northern and north-northeastern sectors. No relationship was observed between groundwater flow direction and calcium concentrations. UNIT 833:2008 does not establish a maximum limit for this parameter.

Data analysis was conducted through the construction of a Piper diagram and an irrigation water classification diagram. According to the Piper diagram, six samples were classified as sodium-bicarbonate waters, three as calcium-bicarbonate waters, and one as magnesium-bicarbonate water (Figure 22). The predominance of sodium ions may be related to cation exchange processes during groundwater evolution. Regarding anionic variation, bicarbonate ions predominate in most samples, while one sample shows a relative increase in chloride ions. The most common cationic pattern follows the sequence $Na^+ + K^+ > Ca^{2+} > Mg^{2+}$, and the anionic pattern $HCO_3^- > SO_4^{2-} + NO_3^- > Cl^-$. Hydrochemical classification indicates that most waters are of the bicarbonate type with low ionic concentrations, suggesting the presence of relatively young groundwater in terms of recharge.

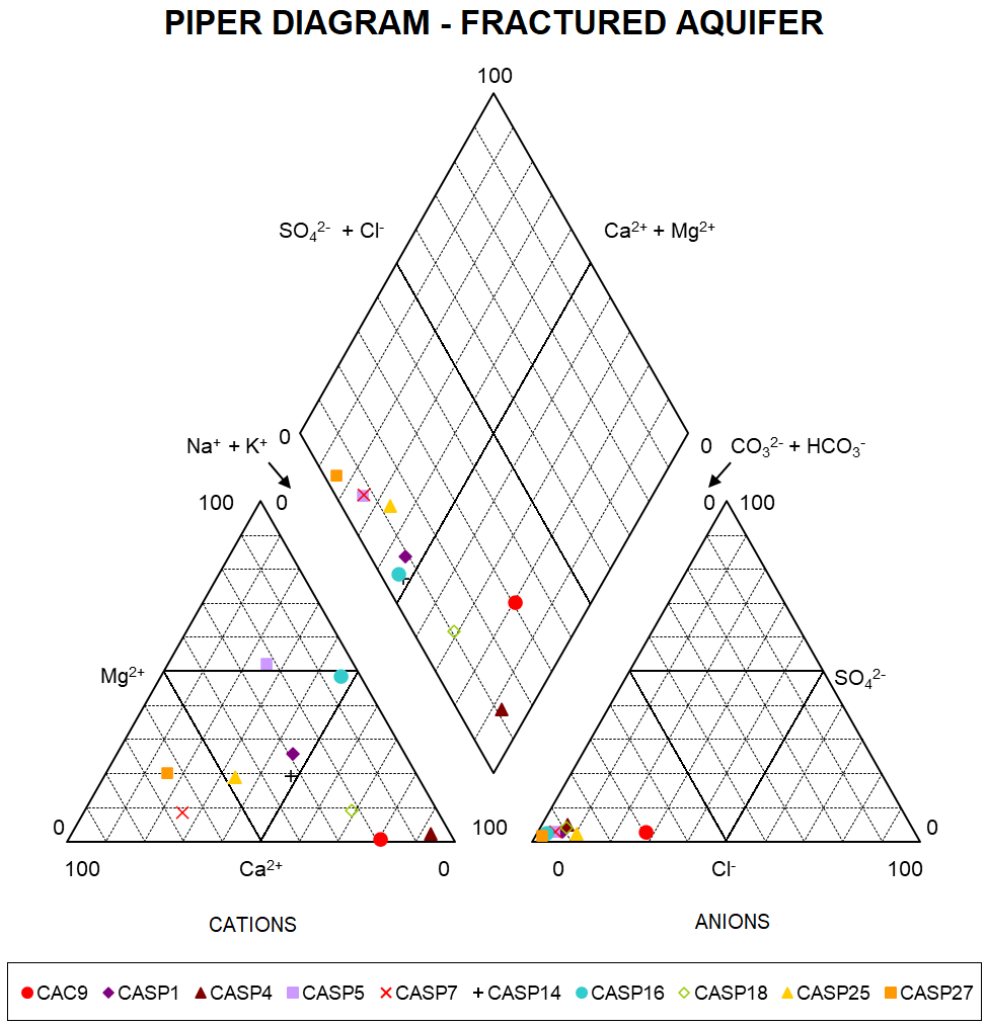

Figure 22. Piper diagram for the fractured aquifer

According to the irrigation water classification diagram, most samples from the fractured aquifer were classified as C3-S1, corresponding to high-salinity, low-sodium waters, suitable for irrigation of well-drained soils and crops with high salinity tolerance (Figure 23).

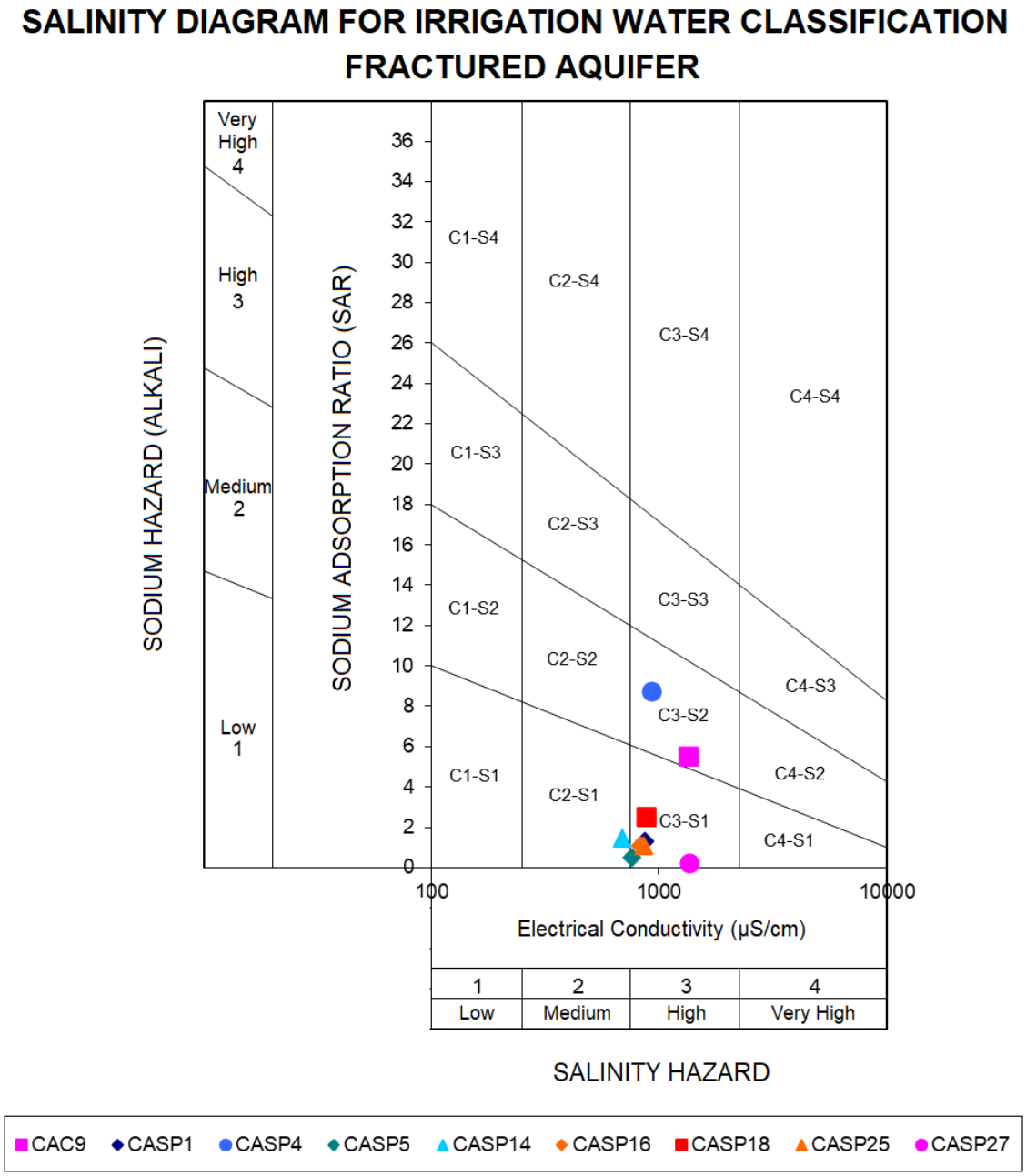

Figure 23. Irrigation water quality classification diagram for the fractured aquifer

In addition to chemical analyses, microbiological parameters were also evaluated. The results showed that total coliforms exceeded the permissible limit (<1 CFU/100 mL) in eight wells (80% of the total samples). Fecal coliforms exceeded this limit in six wells (60%). *Pseudomonas aeruginosa* was not detected (<1 CFU/100 mL), except in two wells, CASP16 and CASP27. Heterotrophic plate counts at 35 °C exceeded the recommended maximum (≤500 CFU/mL) in six wells, with counts ranging from 690 to >2000 CFU/mL, while the remaining four wells were below the limit, with counts between 110 and 440 CFU/mL. The full dataset, including all microbiological parameters determined for each well, is provided in Supplementary Table S9.

3.3.2 Sedimentary Aquifer

Based on the analysis of the measured physicochemical parameters, groundwater generally complied with the standards established for drinking water according to UNIT 833:2008 (UNIT, 2008). However, some samples

exceeded the maximum permissible values. Specifically, two samples from wells CASP13 and CAC2 showed turbidity above the allowable limit, one sample from well CASP9 exceeded the limits for electrical conductivity and total dissolved solids, and one sample from well CAC6 exhibited total hardness above the standard value. The results of the measured physicochemical parameters are presented below and summarized in Table 3, which shows the mean, maximum, and minimum values of groundwater from the sedimentary aquifer. The full dataset, including all parameters measured for each well, is provided in Supplementary Table S4.

Table 3. Mean, maximum, and minimum values of the physicochemical parameters measured in groundwater from the sedimentary aquifer

Physicochemical Parameter	Mean Value	Maximum Value (Well)	Minimum Value (Well)
Electrical Conductivity (µS/cm)	819.23	1296 (CAC7)	472 (CAC8)
pH	7.29	7.58 (CAC5)	6.85 (CASP17)
Redox Potential (Eh) (mV)	197.9	236.5 (CASP17)	165.0 (CAC4)
Dissolved Oxygen (ppm)	4.68	6.65 (CASP11)	2.69 (CASP17)
Total Dissolved Solids (ppm)	409.68	648 (CAC7)	236 (CAC8)
Turbidity (FNU)	0.33	1 (CASP12)	0 (CASP19 y CASP23)
Temperature (°C)	18.48	20.29 (CASP10)	15.35 (CAC6)
Total Hardness (mg/L $CaCO_3$/L)	264.74	480.3 (CASP23)	165.4 (CASP20)

Note. The maximum values of electrical conductivity and total dissolved solids in well CASP9 (2346 µS/cm and 1173 ppm), the maximum turbidity values in wells CASP13 (1.3 FNU) and CAC2 (2.5 FNU), and the maximum total hardness value in well CAC6 (613.8 mg/L as $CaCO_3$) were excluded from the analysis, as all exceed the maximum limits allowed for drinking water.

Electrical Conductivity: The greatest values were recorded in the eastern and central-southern sectors, whereas lower values occurred in the central-western and southern sectors. A decrease in electrical conductivity along the groundwater flow direction was observed. The maximum value (2346 µS/cm, well CASP9), which exceeds the standard, may be influenced by the sediments of the Camacho Formation. Except for this well, all samples were below the maximum permissible limit for drinking water established by UNIT 833:2008 (Figure 24).

pH: Higher values were generally observed in the eastern and southern sectors, associated with elevated topographic areas, while lower values were found in the central-northern sector. The pH range (6.85–7.58) corresponded to neutral conditions. An increasing trend in pH was observed with higher nitrate concentrations, although no apparent relationship with groundwater flow direction was observed. All samples complied with the drinking-water quality range established by UNIT 833:2008 (Figure 25).

Redox Potential (Eh): The highest Eh values were recorded in the central-northern sector, whereas lower values were observed in the central-southern sector. The Eh values also varied slightly but remained positive. No relationship was observed between groundwater flow direction and Eh values.

Dissolved Oxygen: The highest values were found in the north-northwestern and southwestern sectors, while the lowest values were observed in the central sector. No relationship with groundwater flow direction was observed.

Total Dissolved Solids (TDS): The greatest TDS values were recorded in the eastern and central-southern sectors, whereas lower values occurred in the central-western and southern sectors, confirming the relationship with electrical conductivity. A decrease in total dissolved solids along the groundwater flow direction was observed. Except for well CASP9, all samples were below the maximum permissible limit for drinking water established by UNIT 833:2008 (Figure 26).

Turbidity: The highest values were observed in the southern and central-eastern sectors, while the lowest values were found in the central-northern and eastern sectors. No relationship was observed between turbidity and

groundwater flow direction. With the exception of wells CASP13 and CAC2, all samples complied with the maximum permissible limit established by UNIT 833:2008.

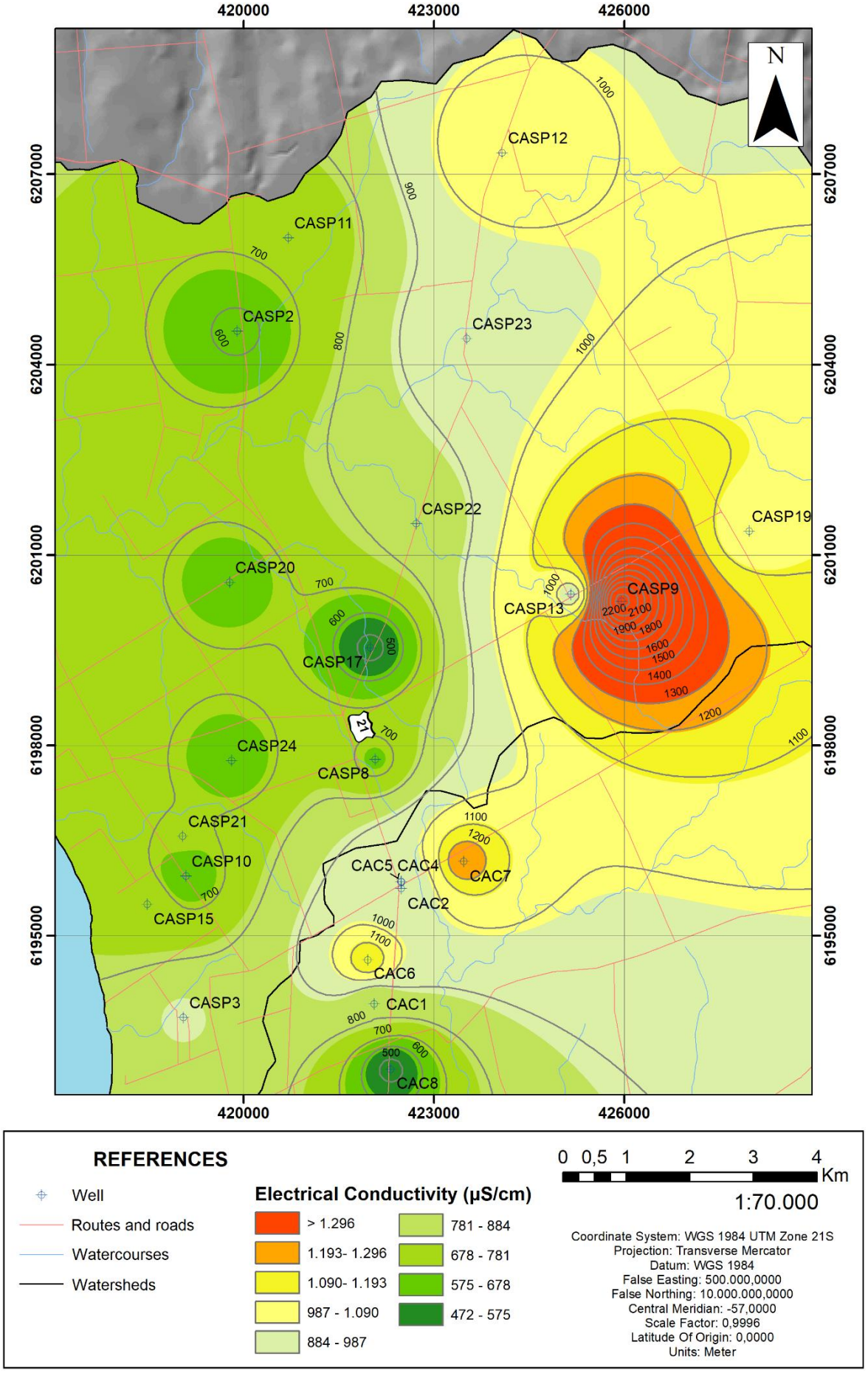

Figure 24. Sedimentary aquifer electrical conductivity map (µS/cm), San Pedro, Colonia

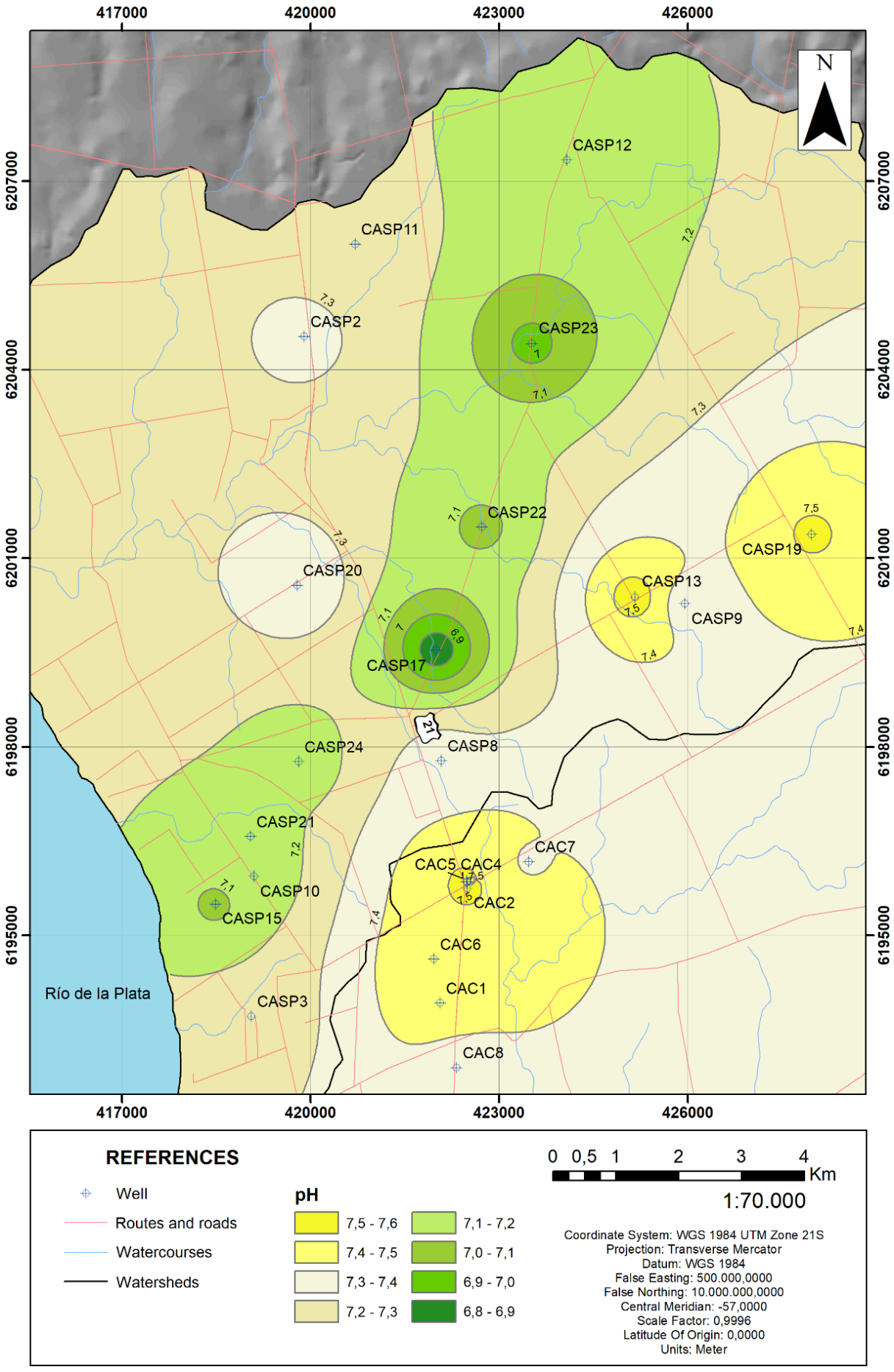

Figure 25. Sedimentary aquifer pH map, San Pedro, Colonia

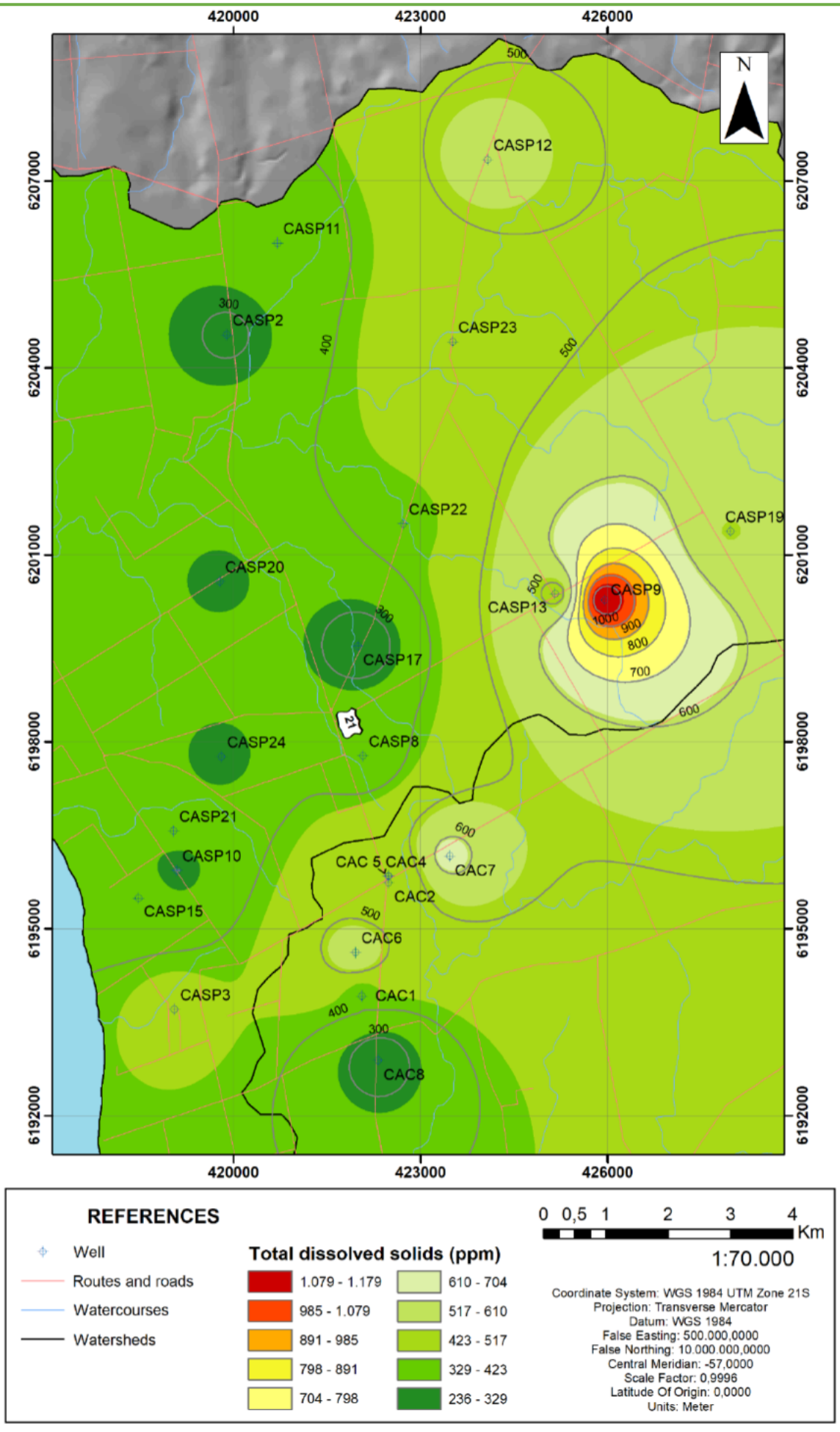

Figure 26. Sedimentary aquifer total dissolved solids map (ppm), San Pedro, Colonia

Temperature: The highest values were recorded in the southwestern and north-northeastern sectors, whereas lower values were observed in the southern and central-western sectors. No relationship with groundwater flow direction was observed. All samples were within the typical temperature range for groundwater.

Total Hardness: Elevated hardness values were observed in the southern and central-northern sectors, while lower values occurred in the western and south-southwestern sectors. No relationship was observed between groundwater flow direction and total hardness values. Based on the mean total hardness, the water was classified as very hard. With the exception of well CAC6, all samples complied with the maximum permissible limit established by UNIT 833:2008.

The analysis of the chemical results indicated that, in general, groundwater complied with the limits established for drinking water according to UNIT 833:2008 (UNIT, 2008). However, some exceptions were detected. Two samples, from wells CAC1 and CAC6, showed nitrate concentrations above the maximum allowable limit, and eight samples exceeded the total arsenic limits. Regarding total arsenic, only two samples, from wells CASP12 and CASP17, were below the guideline value recommended by the WHO (2021). The results of the chemical analyses are summarized in Table 4, which presents the average, maximum, and minimum concentrations of groundwater from the sedimentary aquifer. The full dataset, including all chemical parameters determined for each well, is provided in Supplementary Tables S6, S7 and S8.

Table 4. Mean, maximum, and minimum concentrations of chemical analyses in groundwater from the sedimentary aquifer

Chemical Element	Mean Concentration (mg/L)	Maximum Value (Well) (mg/L)	Minimum Value (Well) (mg/L)
Chlorides (Cl^-)	27.62	107.74 (CAC6)	3.68 (CASP12)
Nitrates (NO_3^-)	18.45	47.75 (CAC7)	0.12 (CAC4)
Bicarbonate (HCO_3^-)	470.13	677.1 (CAC7)	309.88 (CAC3 y CASP24)
Sulfates (SO_4^{2-})	21.59	73.92 (CAC6)	6.86 (CASP17)
Total Arsenic (As)	0.017	0.030 (CAC4)	0.006 (CASP17)
Sodium (Na^+)	39.47	107.77 (CASP9)	7.0 (CAC3)
Potassium (K^+)	7.79	17.38 (CASP22)	0.02 (CASP21)
Magnesium (Mg^{2+})	8.41	19.55 (CASP10)	0.32 (CASP21)
Calcium (Ca^{2+})	10.24	32.32 (CASP22)	1.26 (CAC4)

Note. The maximum nitrate concentrations of 60.55 and 192.68 mg/L, corresponding to wells CAC1 and CAC6, respectively, were excluded from the analysis, as they exceed the maximum limit allowed for drinking water.

Chlorides (Cl^-): The greatest concentrations were observed in the southern sector, whereas lower values occurred in the northern and northeastern sectors. No relationship was observed between groundwater flow direction and chloride concentrations. All samples were below the maximum limit allowed for drinking water according to UNIT 833:2008.

Nitrates (NO_3^-): Elevated concentrations were recorded in the southern sector, while lower values predominated in the northwestern and central-northern sectors, likely associated with semi-confined aquifer conditions. No relationship was detected between groundwater flow direction and nitrate concentrations. With the exception of wells CAC1 and CAC6, all samples complied with the maximum permissible limit for drinking water established by UNIT 833:2008 (Figure 27).

Bicarbonate (HCO_3^-): Higher concentrations were recorded in the southern and central-eastern sectors, whereas lower values were observed in the south-southwestern and southwestern sectors. A decrease in bicarbonate concentrations along the groundwater flow direction was observed. UNIT 833:2008 does not establish a maximum allowable value for this parameter.

Sulfates (SO_4^{2-}): The highest concentrations were found in the southern and south-southeastern sectors, while the lowest occurred in the central-western and southwestern sectors. A decrease in sulfate concentrations along the groundwater flow direction was observed. All samples were below the maximum permissible limit for drinking water established by UNIT 833:2008.

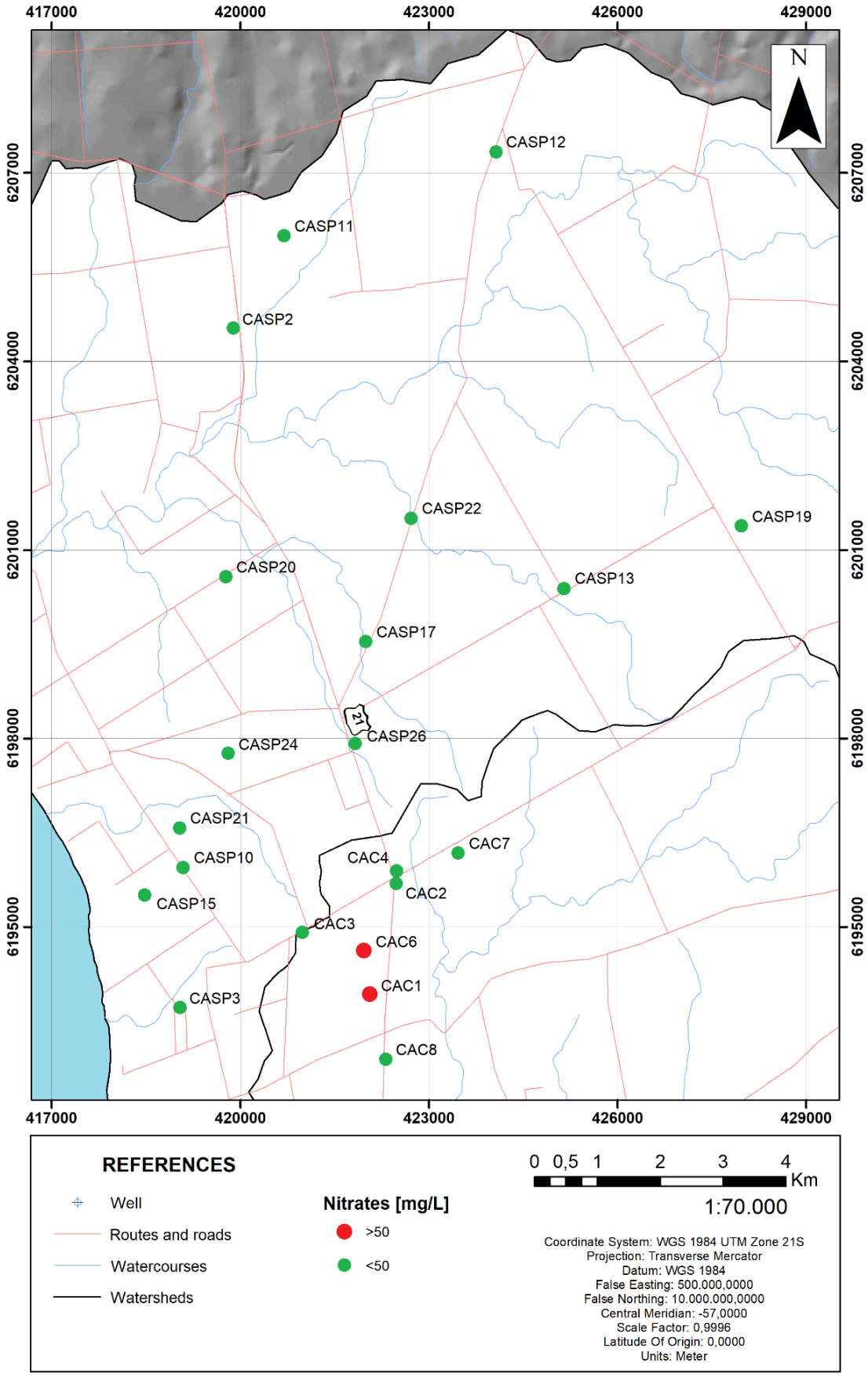

Figure 27. Sedimentary aquifer groundwater nitrates concentration map [mg/L], San Pedro, Colonia

Total Arsenic (As): Elevated total arsenic concentrations are related to both natural and anthropogenic processes. An increasing trend in total arsenic concentration was observed with higher nitrate concentrations, possibly associated with agricultural activities. The anomalously high total arsenic concentration was recorded in the southern sector, while the lowest concentration was observed in the central sector. No relationship with groundwater flow direction was detected. Eight samples exceeded the maximum limit established by UNIT 833:2008, whereas two samples, from wells CASP12 and CASP17, were below the guideline value suggested by the WHO (2021) (Figure 28).

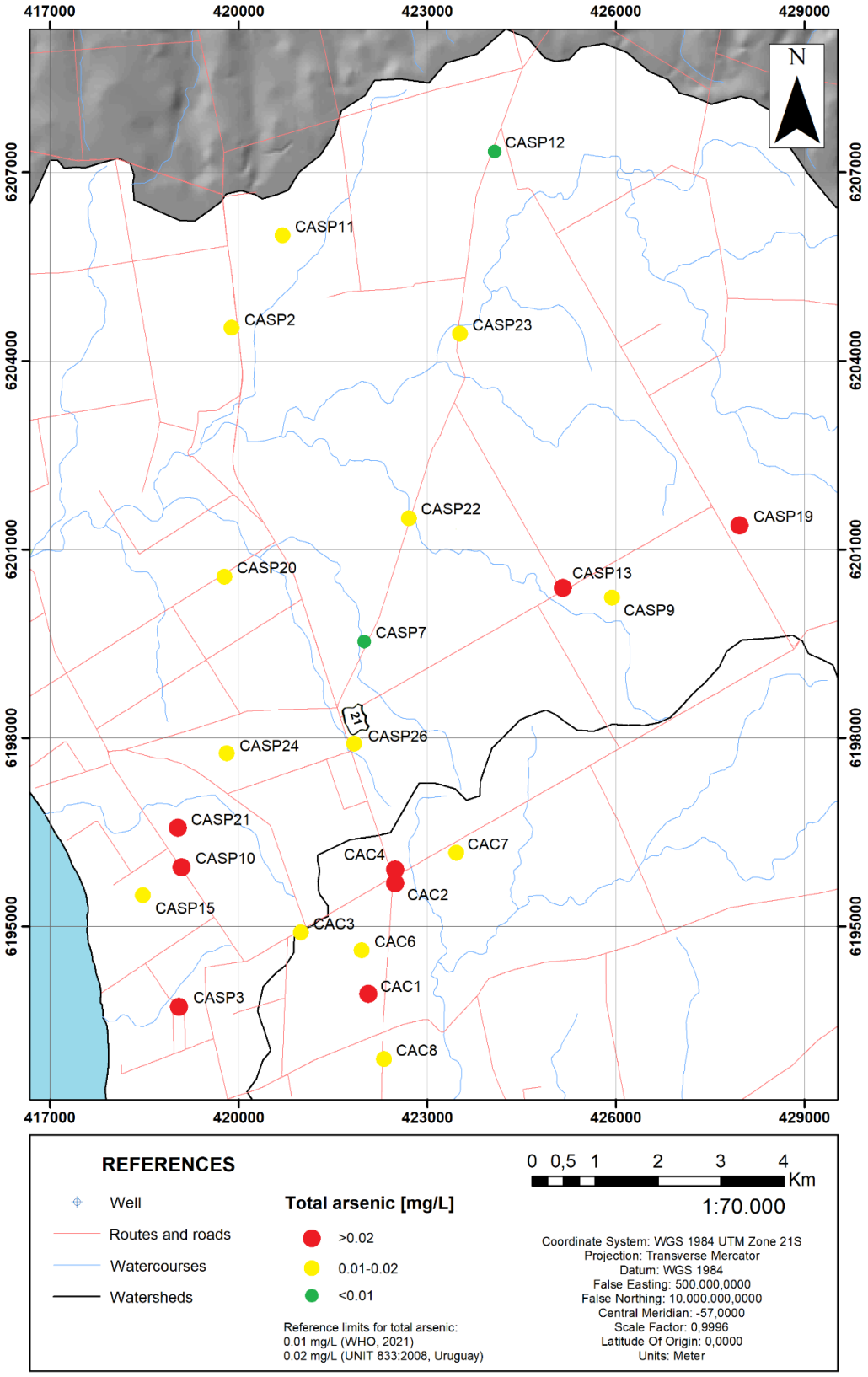

Figure 28. Sedimentary aquifer groundwater total arsenic concentration map [mg/L], San Pedro, Colonia

Sodium (Na^+): The highest concentrations were found in the eastern and south-southeastern sectors, whereas the lowest values occurred in the south-southwestern and west-southwestern sectors. A decreasing trend in sodium concentrations along the groundwater flow direction was observed. All samples were below the maximum limit for drinking water established by UNIT 833:2008.

Potassium (K^+): Elevated concentrations were recorded in the central and north-northwestern sectors, while lower values were observed in the west-southwestern and south-southeastern sectors. No relationship with groundwater flow direction was observed. According to UNIT 833:2008, no maximum allowable value is established for this parameter.

Magnesium (Mg^{2+}): Higher concentrations were observed in the southwestern and central sectors, whereas lower concentrations occurred in the west-southwestern and south-southeastern sectors. No relationship was observed between groundwater flow direction and magnesium concentrations. For this parameter, UNIT 833:2008 does not establish a maximum allowable value for drinking water quality.

Calcium (Ca^{2+}): The highest concentrations were recorded in the central and southwestern sectors, while the lowest concentrations were found in the southern and south-southeastern sectors. No relationship was observed between groundwater flow direction and calcium concentrations. For this parameter, UNIT 833:2008 does not establish a maximum allowable value for drinking water quality.

Data analysis was performed using a Piper diagram and an irrigation water classification diagram. According to the Piper diagram, 15 samples were classified as sodium-bicarbonate waters, 4 as calcium-bicarbonate waters, and 2 as magnesium-bicarbonate waters (Figure 29). The predominance of sodium ions could be associated with cation exchange processes during the natural evolution of groundwater. Regarding anionic variation, bicarbonate ions predominated in most samples, while one sample showed an elevated chloride ion concentration compared to the others. The most frequent cationic pattern follows the sequence $Na^+ + K^+ > Ca^{2+} > Mg^{2+}$, while the anionic pattern is $HCO_3^- > SO_4^{2-} + NO_3^- > Cl^-$. Hydrochemical classification indicates that most waters are of the bicarbonate type with low ionic concentrations, suggesting they are relatively young in terms of recharge.

According to the irrigation water classification diagram, most samples from the sedimentary aquifer were classified as C3-S1 and C2-S1, corresponding to waters with high to medium salinity and low sodium content. These waters are suitable for irrigation of well-drained soils and for crops with high salinity tolerance (Figure 30).

In addition to the chemical analyses, microbiological determinations were performed. The results showed that total coliforms exceeded the permissible limit (<1 CFU/100 mL) in 14 wells (63.6%), and fecal coliforms exceeded the limit (<1 CFU/100 mL) in seven wells (31.8%). *Pseudomonas aeruginosa* was not detected (<1 CFU/100 mL) in most samples, except in three wells (CASP2, CASP10, and CASP20). Heterotrophic plate counts at 35 °C exceeded the recommended maximum (≤500 CFU/mL) in 14 wells, with counts ranging from 660 to >2000 CFU/mL, whereas the remaining eight wells were below the limit, with counts between 50 and 400 CFU/mL. The full dataset, including all microbiological parameters determined for each well, is provided in Supplementary Table S10.

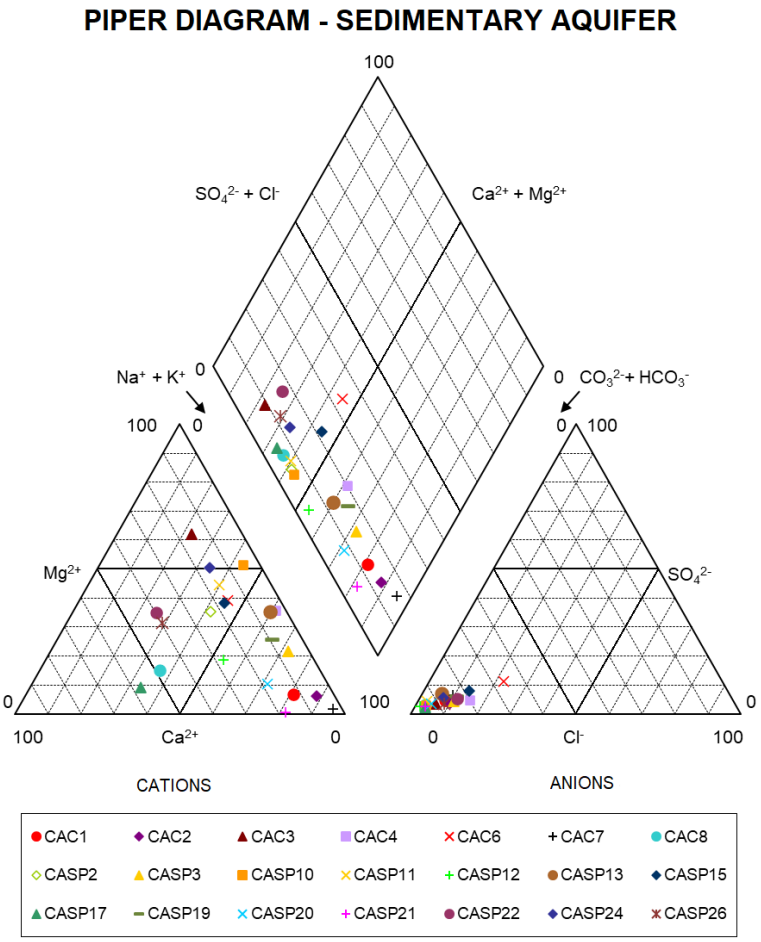

Figure 29. Piper diagram for the sedimentary aquifer

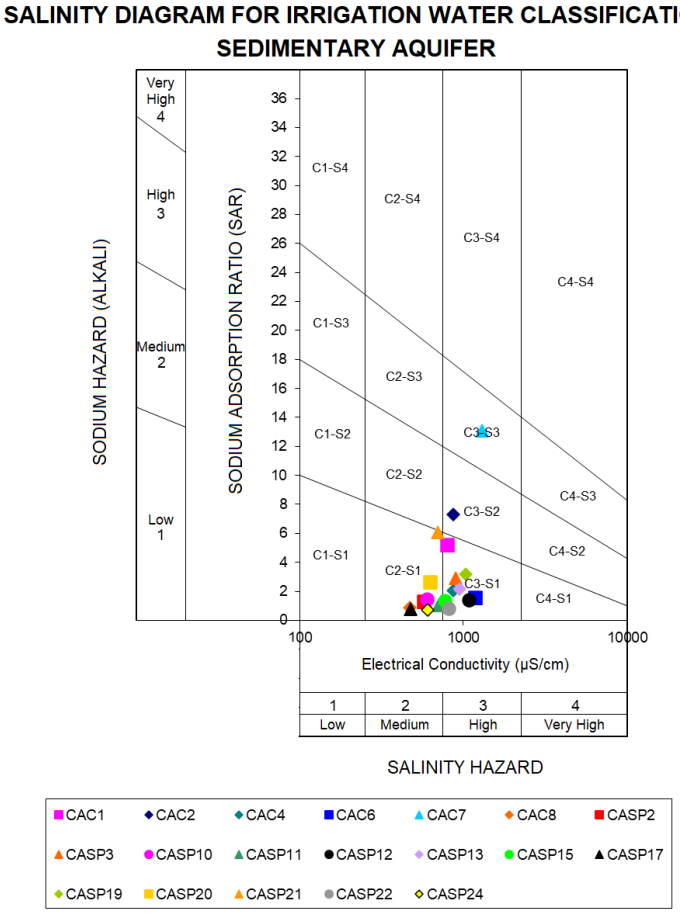

Figure 30. Irrigation water quality classification diagram for the sedimentary aquifer

4. Discussion

In the fractured aquifer, a trend of increasing pH is observed with rising nitrate concentrations. This relationship can be explained by the infiltration of surface waters enriched in nitrates, originated from agricultural activities or nearby septic wells. The increase in pH can be attributed both to the surface input of cations and bicarbonate associated with anthropogenic infiltration, and to the release of cations through the weathering of primary granite minerals. Both processes contribute to the consumption of H^+ in solution, promoting more alkaline conditions in the aquifer.

In turn, a decrease in pH was observed along the groundwater flow direction, attributable both to mineral dissolution and to CO_2 production from microbial activity, which forms carbonic acid upon dissolution in water (Feth et al., 1964; Pedersen, 1997). In addition, dissolved oxygen was observed to decline along the groundwater flow, due to both geochemical reactions and biological consumption by heterotrophic bacteria (Ben Maamar et al., 2015; Bochet et al., 2020; Pedersen, 1997; Sahl et al., 2008; Samper et al., 2003). Similarly, a decrease in bicarbonate was observed along the groundwater flow, likely associated with reduced surface recharge, which lowers the availability of dissolved CO_2 in the water. As groundwater moves away from recharge areas, it contains less carbonic acid, limiting the dissolution of silicate minerals in the granite and, consequently, reducing the input of HCO_3^- to the water (Appelo & Postma, 2005; Stober et al., 2022). Finally, a decrease in sodium concentration was observed along the groundwater flow direction, suggesting the occurrence of direct cation exchange processes. Although negative values of the Chloro-Alkaline Index (CAI-1 and CAI-2) (Schoeller, 1977) indicate that direct cation exchange predominates, in which Ca^{2+} and Mg^{2+} are adsorbed onto clays minerals and Na^+ is released into the water, the high hardness observed suggests that additional processes, such as mixing with more mineralized waters, weathering of feldspars and micas, or prolonged residence times, also contribute significantly to Ca^{2+} and Mg^{2+} concentrations in the aquifer (Gugulothu et al., 2022).

In the sedimentary aquifer, a trend of increasing pH was observed with increasing nitrate concentrations, similar to that recorded in the fractured aquifer. Conversely, along the groundwater flow path, a decrease in electrical conductivity and total dissolved solids was observed. This trend could be related to mixing with recently recharged waters, which are generally less mineralized and dilute the concentrations of ions along the groundwater flow, and to possible carbonate precipitation in the Raigón Formation. Carbonate precipitation would occur if local conditions are favorable for the removal of Ca^{2+} and dissolved inorganic carbon (Dirección Nacional de Minería y Geología, 2024; Freeze & Cherry, 1979; Plata Bedmar et al., 2003; Santos et al., 2019).

On the other hand, a decrease in bicarbonate was observed along the groundwater flow direction, possibly due to reduced surface recharge and, consequently, diminished dissolved CO_2. As groundwater moves away from recharge areas, it contains less carbonic acid, limiting the dissolution of minerals in the sandstones and clays of the Raigón Formation, reducing the input of HCO_3^- to the water and/or favoring its precipitation (Appelo & Postma, 2005; Dirección Nacional de Hidrografía et al., 2005). The observed decrease in sulfates along the flow path is likely explained by microbial sulfate-reduction processes under relatively reducing conditions (Chapelle, 1993; Miao et al., 2012). Finally, a decrease in sodium concentration was observed along the flow path, suggesting the occurrence of direct cation exchange processes. Negative values of the Chloro-Alkaline Index (CAI-1 and CAI-2) (Schoeller, 1977) indicate that this type of exchange predominates, whereby Ca^{2+} and Mg^{2+} are adsorbed onto the clays of the Raigón Formation and Na^+ is released into the water. However, the observed high hardness suggests that additional processes, such as weathering of feldspars, mixing with more mineralized waters, or prolonged interaction with sediments, also contribute substantially to Ca^{2+} and Mg^{2+} concentrations in the aquifer (Arroyo-Figueroa et al., 2024; Dirección Nacional de Hidrografía et al., 2005; Freeze & Cherry, 1979).

Results indicate that in some wells, both aquifers exhibit nitrate concentrations exceeding the limits established by UNIT 833:2008, likely due to agricultural activities and inadequate effluent management. High levels of total and fecal coliforms, associated with the proximity of wells to residences or dairy farms, also indicate a major route of anthropogenic contamination.

In the case of total arsenic, considering both aquifers, 27% of the wells exceed the UNIT 833:2008 standard, and 91% of the wells exceed the WHO recommended concentration. These elevated concentrations could be related to water infiltration through the Libertad Formation, which contributes arsenic to the underlying aquifers. Overall, the results highlight the need to improve water management practices to ensure the quality and sustainability of water resources and to reduce risks to human health.

5. Conclusions

Two aquifer units were identified in the study area, one composed of granites of the Crystalline Basement, forming a fractured aquifer, and another composed of the Raigón Formation, forming a sedimentary aquifer.

In the fractured aquifer, the May 2021 piezometric measurements indicated a predominant groundwater flow in a southeast-northwest direction. The piezometric surface exhibited a relatively flat pattern, with a slight radial divergence in the central-eastern sector, suggesting the presence of a recharge area. Hydraulic gradients were higher in the central-western and southwestern sectors, possibly indicating natural discharge areas of the aquifer. In the central-southern sector, relatively uniform hydraulic gradients were observed.

In general, the groundwater met the drinking water standards established by UNIT 833:2008 (UNIT, 2008), although some exceptions were observed. Turbidity values in wells CASP27 and CAC9 exceeded the maximum allowable limit. Additionally, nitrate concentrations in well CASP25 and total arsenic in well CASP4 exceeded the regulatory limits, while only well CASP5 presented total arsenic below the WHO (2021) recommended value.

In the sedimentary aquifer, the May 2021 piezometric measurements indicated a general groundwater flow in a southeast-northwest direction in the northern sector and a northeast-southwest direction in the southern sector. In the western sector, the piezometric surface exhibited a convergent radial pattern at its northeastern end and a divergent radial pattern at its southeastern end, with hydraulic gradients of 0.003 and 0.005, suggesting a discharge area with flow directed westward, toward the San Pedro Creek. In the eastern sector, a convergent radial pattern and a hydraulic gradient of 0.004 were observed, which could indicate a recharge area. In the central sector, between both domains, hydraulic gradients were low in the northern and central parts, and higher in the southern part, suggesting a discharge zone in the latter case.

In general, the groundwater met the drinking water standards established by UNIT 833:2008 (UNIT, 2008), although some exceptions were observed. Wells CASP13 and CAC2 exceeded the turbidity limit, well CASP9 exceeded electrical conductivity and total dissolved solids, and well CAC6 showed total hardness above the regulatory value. Additionally, nitrate concentrations in wells CAC1 and CAC6, and total arsenic in eight wells, exceeded the regulatory limits, while only two samples, from wells CASP12 and CASP17, showed total arsenic below the WHO (2021) recommended value.

The piezometric analysis of both aquifers indicated that the predominant flow is from southeast to northwest, with recharge areas in the central-eastern sector and discharge areas in the central-western sector. Additionally, it is suggested that the recharge zones of the sedimentary aquifer could contribute to the recharge of the fractured aquifer.

Considering both aquifers, the groundwater is classified as sodium-calcium bicarbonate type. High concentrations of nitrates and total and fecal coliforms are associated with inadequate water and soil management practices, mainly linked to dairy farming activities, affecting a large part of the study area. In the western and southwestern sectors, nitrate and coliform concentrations are low. High arsenic concentrations, on the other hand, could be related to the lithology of the geological units forming the aquifers.

According to the groundwater classification diagram for irrigation, most samples from the fractured aquifer fall into category C3-S1, indicating high salinity and low sodium content. In the sedimentary aquifer, most samples correspond to C3-S1 and C2-S1, reflecting high to medium salinity and low sodium content. The elevated salinity observed in both aquifers may be attributed to the dissolution of minerals present in granites and sandstones, as well as the influence of agricultural activities that contribute salts to the subsurface. Overall, the groundwater is suitable for irrigation in well-drained soils and for crops that are highly tolerant to salinity.

A continuous monitoring program for physicochemical and microbiological parameters should be implemented for all wells, with particular attention to those exceeding regulatory limits. Wellhead protection zones with specified radii should be established and maintained around wells to prevent infiltration of contaminants from agricultural, livestock, or domestic sources, and to ensure proper well construction and maintenance. Good agricultural and livestock management practices should be promoted to minimize discharge of effluents from dairy farms and domestic sources into the aquifer. In addition, training and awareness programs involving producers, local communities, and municipal authorities should be developed to emphasize the importance of protecting the water resource and promoting its sustainable use.

Acknowledgements

We would like to thank the Cooperativa Agraria Suplementada San Pedro (CASSPE) for their primary financial support.

Transparency of Data

Available data: The entire data set that supports the results of this study was published in the article itself.

Author Contribution Statement

	V Strambini	P Collazo
Conceptualization	■	■
Data curation	■	
Formal analysis	■	
Investigation	■	■
Supervision		■
Visualization	■	
Writing – original draft	■	
Writing – review and editing	■	

References

American Public Health Association; American Water Works Association & Water Environment Federation. (1998). *Standard methods for the examination of water and wastewater* (20th ed.).

American Public Health Association; American Water Works Association & Water Environment Federation. (2017). *Standard methods for the examination of water and wastewater* (23rd ed.).

Appelo, C. A. J., & Postma, D. (2005). *Geochemistry, groundwater and pollution* (2nd ed.). CRC Press.

Arroyo-Figueroa, C., Chalá, D. C., Gutiérrez-Ribon, G., & Quiñones-Bolaños, E. (2024). A framework to evaluate groundwater quality and the relationship between rock weathering and groundwater hydrogeochemistry in the tropical zone: A case study of coastal Aquifer Arroyo Grande, in the Caribbean Region of Colombia . *Water, 16*(12), Article 1650. https://doi.org/10.3390/w16121650

Ben Maamar, S., Aquilina, L., Quaiser, A., Pauwels, H., Michon-Coudouel, S., Vergnaud-Ayraud, V., Labasque, T., Roques, C., Abbott, B. W., & Dufresne, A. (2015). Groundwater isolation governs chemistry and microbial community structure along hydrologic flowpaths. *Frontiers in Microbiology*, *6*, Article 1457. https://doi.org/10.3389/fmicb.2015.01457

Bochet, O., Bethencourt, L., Dufresne, A., Farasin, J., Pédrot, M., Labasque, T., Chatton, E., Lavenant, N., Petton, C., Abbott, B. W., Aquilina, L., & Le Borgne, T. (2020). Iron-oxidizer hotspots formed by intermittent oxic–anoxic fluid mixing in fractured rocks. *Nature Geoscience, 13*, 149-155. https://doi.org/10.1038/s41561-019-0509-1

Bossi, J., & Ferrando, L. (2001). *Carta geológica del Uruguay a escala 1:500,000*. Universidad de la República.

Chapelle, F. H. (1993). *Ground-water microbiology and geochemistry*. John Wiley & Sons.

Cicalese, H. (1998). *Estudio geofísico: diagnóstico para obtención de agua subterránea: Poblado San Pedro*. MEVIR.

Dirección Nacional de Hidrografía; Dirección Nacional de Medio Ambiente; Dirección Nacional de Minería y Geología; Dirección General de Recursos Naturales Renovables; Obras Sanitarias del Estado, & Facultad de Ciencias. (2005). *Gestión sostenible del Acuífero Raigón Uruguay*: *Manejo integrado y sostenible de aguas subterráneas en América Latina*. https://inis.iaea.org/records/a91je-kzy39/files/41076192.pdf?download=1

Dirección Nacional de Minería y Geología. (2024). *Síntesis del conocimiento sobre el Sistema Acuífero Raigón: Geología, hidrogeología e hidroquímica*. MIEM. https://www.gub.uy/ministerio-industria-energia-mineria/comunicacion/publicaciones/sintesis-del-conocimiento-sobre-sistema-acuifero-raigon-sar

Feth, J. H., Roberson, C. E., & Polzer, W. L. (1964). *Sources of mineral constituents in water from granitic rocks, Sierra Nevada, California and Nevada*. U.S. Geological Survey. https://pubs.usgs.gov/wsp/1535i/report.pdf

Freeze, R. A., & Cherry, J. A. (1979). Chemical evolution of natural groundwater. In R. A. Freeze & J. A. Cherry (Eds.), *Groundwater* (pp. 237-302). Prentice-Hall.

Gianotti, V., & Arrighetti, R. (2017). [Mapa geológico de las Hojas Rosario (83) y Colonia (91) a escala 1:100,000]. In *Proyecto cartografía geocientífica del Uruguay.* MIEM. https://www.gub.uy/ministerio-industria-energia-mineria/comunicacion/publicaciones/carta-geologica-escala-1100000-hojas-83-91-colonia

Goso, H. (1965). *El Cenozoico en el Uruguay*. Instituto Geológico del Uruguay.

Goso, H., & Bossi, J. (1966). Cenozoico. In J. Bossi (Ed.), *Geología del Uruguay* (pp. 259-305). Universidad de la República.

Goso Aguilar, C., & Muzio, R. (2006). Geología de la costa uruguaya y sus recursos minerales asociados. In R. Menafra, L. Rodríguez-Gallego, F. Scarabino & D. Conde (Eds.), *Bases para la conservación y el manejo de la costa uruguaya* (pp. 9-20). Vida Silvestre Uruguay.

Gugulothu, S., Subbarao, N., Das, R., & Dhakate, R. (2022). Geochemical evaluation of groundwater and suitability of groundwater quality for irrigation purpose in an agricultural region of South India. *Applied Water Science, 12*, Article 142. https://doi.org/10.1007/s13201-022-01583-w

Heinzen, W., Carrión, R., Massa, E., Pena, S., & Stapff, M. (2003). *República Oriental del Uruguay: Mapa hidrogeológico a escala 1:1,000,000*. MIEM.

Instituto Uruguayo de Normas Técnicas. (2008). *Agua potable: Requisitos* (UNIT 833:2008).

Martínez, S., & Ubilla, M. (2009). El Cuaternario en Uruguay. In G. Veroslavsky, M. Ubilla & S. Martínez (Eds.), *Cuencas sedimentarias de Uruguay: Geología, paleontología y recursos naturales: Vol. 5 Cenozoico* (pp. 195-227). Universidad de la República.

Menéndez, M. (2017). *Manual de procedimientos analíticos para muestras ambientales: 1002UY: Determinación de alcalinidad en aguas naturales, residuales, residuales tratadas y aguas de lluvia* (3rd ed.). Ministerio de Ambiente.

Miao, Z., Brusseau, M. L., Carroll, K. C., Carreón-Diazconti, C., & Johnson, B. (2012). Sulfate reduction in groundwater: Characterization and applications for remediation. *Environmental Geochemistry and Health*, *34*(4), 539-550. https://doi.org/10.1007/s10653-011-9423-1

Montaño, J. (1999). *Caracterización y vulnerabilidad de sistemas hidrogeológicos discontinuos: Cuenca del Arroyo Carrasco – Montevideo – Uruguay* [Doctoral dissertation]. Universidad de Buenos Aires.

Pedersen, K. (1997). Microbial life in deep granitic rock. *FEMS Microbiology Reviews, 20*(3-4), 399-414. https://doi.org/10.1016/S0168-6445(97)00022-3

Perea, D., & Martínez, S. (2009). Estratigrafía del Mioceno-Pleistoceno en el litoral Sur-Oeste de Uruguay. In G. Veroslavsky, M. Ubilla & S. Martínez (Eds.), *Cuencas sedimentarias de Uruguay: Geología, paleontología y recursos naturales: Vol. 5 Cenozoico* (pp. 105-124). Universidad de la República.

Plata Bedmar, A., Dellepere, A., Roma, M. T., & Garat, S. (2003). Determinación de la recarga del acuífero Raigón (Uruguay) a partir del tritio natural. *Ingeniería Civil*, (132), Article 127. https://ingenieriacivil.cedex.es/index.php/ingenieria-civil/article/view/1792

Postiglione, M., Batista, L., Costa, D., Chao, R., Gorfain, J., Ledesma, J., Pérez, F., Sordo, A., Vignale, D., Carrión, R., Masa, E., Pena, S., Stapff, M., Bico, J., Caristo, R., Decoud, P., Roma, M. T., Guerèquiz, R., Montaño, J., & Peel, E. (2009). Gestión sostenible del Acuífero Raigón, Uruguay. In *Estudios de hidrología isotópica en América Latina 2006* (pp. 195-218). IAEA.

Preciozzi, F., Spoturno, J., Heinzen, W., & Rossi, P. (1985). *Memoria explicativa de la Carta Geológica del Uruguay a escala 1:500,000*. Ministerio de Industria y Energía.

Rodríguez, R., Bango, G., Flaquer, A., & Musso, M. (2017). Propiedades hidráulicas de la Fm. Libertad: Ensayos de campo y laboratorio. In *Actas del XX Congreso Argentino de Geología* (pp. 35-39). Asociación Geológica Argentina.

Sahl, J. W., Schmidt, R., Swanner, E. D., Mandernack, K. W., Templeton, A. S., Kieft, T. L., Smith, R. L., Sanford, W. E., Callaghan, R. L., Mitton, J. B., & Spear, J. R. (2008). Subsurface microbial diversity in deep-granitic-fracture water in Colorado. *Applied and Environmental Microbiology*, *74*(1), 143-152. https://doi.org/10.1128/AEM.01133-07

Samper, J., Molinero, J., Yang, C., & Zhang, G. (2003). *Redox zone II: Coupled modeling of groundwater flow, solute transport, chemical reactions and microbial processes in the Äspö island* (Technical Report TR-03-16). Svensk Kärnbränslehantering AB. https://skb.com/publication/21409

Santos, J. E. de los, Custodio Gimena, E., Flaquer Barrios, A. N., Giménez Martínez, M. C., Menta Romano, A., & Bessouat Ferraris, C. (2019). *Gestión ambiental del Sistema Acuífero Raigón*. INIA. https://ainfo.inia.uy/digital/bitstream/item/13022/1/Inia-Fpta-78-proyecto-307-2019.pdf

Schoeller, H. (1977). Geochemistry of groundwater. In *Groundwater studies: An international guide for research and practice* (pp. 1-18). UNESCO.

Sprechmann, P., Martínez, S., & Gaucher, C. (1994). Paleoecología y sedimentología de la Formación Camacho en el Departamento de Colonia (Mioceno Medio-Superior, Uruguay). In *I Jornada de Paleontología del Uruguay "Prof. Dr. Rodolfo Méndez-Alzola"* (pp. 21-24). Universidad de la República.

Stober, I., Giovanoli, F., Wiebe, V., & Bucher, K. (2022). Deep hydrochemical section through the Central Alps: Evolution of deep water in the continental upper crust and solute acquisition during water–rock-interaction along the Sedrun section of the Gotthard Base Tunnel. *Swiss Journal of Geosciences, 115*, Article 9. https://doi.org/10.1186/s00015-022-00413-0

Strambini Ruiz, M. V. (2023). *Vulnerabilidad y caracterización hidrogeoquímica de las aguas subterráneas de la Cuenca del Arroyo San Pedro y Cuenca del Arroyo de la Caballada, San Pedro, Colonia* [Bachelor's thesis]. Universidad de la República.

Ubilla, M., & Martínez, S. (2016). *Geology and paleontology of the Quaternary of Uruguay*. Springer.

Ugalde, R. A. (2019). *Petrografía, quimioestratigrafía y proveniencia sedimentaria de la Formación Camacho (Mioceno), Uruguay* [Master's thesis]. Universidad de la República.

World Health Organization. (2021). *A global overview of national regulations and standards for drinking-water quality*.

Supplementary Material

Complementary Data Tables

Table S1. Well inventory of the fractured aquifer

Code	X	Y	Z (m)	Static level (m)	Total well depth (m)	Flow rate (m³/h)	Uses
CAC9	425797.4	6194806.16	46	Sealed	-	-	D
CASP1	426065.23	6202010.33	46	1.31	40.0	12.0	D, T
CASP4	427011.41	6207479.6	52	19.17	48.0	5.5	T
CASP5	423772.95	6203700.63	22	0.78	40.0	10.0	D, T
CASP6	421917.95	6197724.96	31	2.22	20.0	5.0	I
CASP7	422098.57	6197786.54	38	7.23	40.0	4.0	D
CASP14	430148.05	6201090.81	68	Sealed	34.0	10.0	D, T
CASP16	425422.53	6204371.29	41	6.98	32.0	6.5	D, T
CASP18	421678.44	6197772.55	34	9.87	28.0	12.0	D, T
CASP25	426346.33	6209162.44	47	Sealed	-	3.0	D
CASP27	421851.25	6198399.64	38	Sealed	-	-	D

*D: domestic, T: dairy farms, R: irrigation

Table S2. Well inventory of the sedimentary aquifer

Code	X	Y	Z (m)	Type of well	Static level (m)	Total well depth (m)	Flow rate (m³/h)	Uses
CAC1	422058.56	6193922.37	39	Walled	19.77	27.36	-	D
CAC2	422487.51	6195742.2	45	Walled	7.73	-	-	D
CAC3	421002.17	6194911.56	26	Semi-artesian	8.67	-	-	D, T
CAC4	422489.68	6195849.41	49	Semi-artesian	9.28	27.0	1.8	D
CAC5	422478.68	6195852.1	49	Walled	9.49	12.54	-	D
CAC6	421958.23	6194620.8	29	Walled	7.83	12.53	-	D
CAC7	423467.58	6196170.77	59	Walled	16.53	21.02	-	D, T
CAC8	422321.22	6192893.22	16	Walled	1.69	3.90	-	D
CASP2	419897.65	6204531.08	60	Semi-artesian	Sealed	-	-	D, T
CASP3	419052.98	6193711.31	29	Walled	5.53	6.97	2.0	D, T
CASP8	422078.21	6197776.82	21	Walled	6.30	11.22	-	D
CASP9	425953.48	6200276.4	37	Walled	12.26	14.51	0.7	D, T
CASP10	419092.88	6195940.71	17	Semi-artesian	Sealed	31.0	-	D, T
CASP11	420706.36	6206000.56	22	Semi-artesian	Sealed	18.0	5.0	D, T
CASP12	424076.26	6207340.14	61	Walled	12.16	14.04	-	D, T
CASP13	425157.18	6200379.1	32	Walled	9.10	13.36	-	D, T
CASP15	418481.97	6195496.42	39	Semi-artesian	9.50	34.0	3.6	D, T
CASP17	422001.17	6199537.59	43	Walled	3.86	5.84	-	T
CASP19	427970.06	6201379.24	53	Semi-artesian	8.15	37.0	3.0	D, T
CASP20	419781.06	6200570.77	25	Semi-artesian	5.19	32.0	6.0	D, T
CASP21	419040.67	6196571.15	23	Semi-artesian	Sealed	15.0	-	D, T
CASP22	422722.13	6201496.89	29	Semi-artesian	2.64	32.0	-	D, T
CASP23	423516.59	6204415.66	24	Semi-artesian	Sealed	26.0	2.5	D, T
CASP24	419809.51	6197762.85	31	Semi-artesian	Sealed	18.0	-	D, T
CASP26	421837.24	6197906.04	33	Walled	-	-	-	D, T

*D: domestic, T: dairy farms.

Table S3. Results of physicochemical parameters of groundwater from the fractured aquifer

Code	pH	Eh (mV)	Dissolved Oxygen (ppm)	Electrical Conductivity (µS/cm)	Total Dissolved Solids (ppm)	Turbidity (FNU)	Temperature (°C)
CAC9	7.29	143.7	3.52	1338	669	1.6	14.18
CASP1	7.13	214.4	5.01	870	435	0.4	18.58
CASP4	7.40	180.5	4.75	929	466	0.4	14.64
CASP5	6.91	215.1	3.67	764	382	0.1	19.03
CASP6	7.19	190.8	3.19	829	414	1.0	18.89
CASP14	7.30	224.6	4.47	691	346	0.1	16.31
CASP16	7.36	207.1	5.10	831	416	0	17.88
CASP18	7	210.1	3.08	880	440	0	19.01
CASP25	7.11	192.6	6.50	863	432	0.2	17.21
CASP27	7.34	140.3	2.71	1365	685	1.4	14.51

Table S4. Results of physicochemical parameters of groundwater from the sedimentary aquifer

Code	pH	Eh (mv)	Dissolved Oxygen (ppm)	Electrical Conductivity (µS/cm)	Total Dissolved Solids (ppm)	Turbidity (FNU)	Temperature (°C)
CAC1	7.48	186.9	4.76	796	398	0.4	18.76
CAC2	7.52	169.3	4.54	871	436	2.5	16.56
CAC4	7.43	165.0	3.58	867	433	0.2	18.85
CAC5	7.58	184.6	3.82	1092	546	0.2	18.1
CAC6	7.48	169.1	5.00	1181	590	0.3	15.35
CAC7	7.39	188.2	3.94	1296	648	0.3	19.36
CAC8	7.34	193.2	3.42	472	236	0.7	18.54
CASP2	7.33	205.6	3.80	575	288	0.1	18.76
CASP3	7.22	205.7	5.04	899	450	0.5	17.93
CASP8	7.35	176.5	4.54	665	333	0.1	19.16
CASP9	7.37	214.4	5.56	2346	1173	0.4	18.33
CASP10	7.13	201.3	6.14	599	299	0.8	20.29
CASP11	7.24	201	6.65	702	351	0.1	18.15
CASP12	7.11	235.9	3.31	1082	542	1.0	19.31
CASP13	7.54	194.2	5.49	945	472	1.3	18.84
CASP15	7.08	184.6	5.59	768	384	0.8	18.69
CASP17	6.85	236.5	2.69	474	238	0.2	18.1
CASP19	7.51	196.7	5.18	1030	515	0	18.95
CASP20	7.40	196.5	4.83	628	314	0.1	17.05
CASP21	7.15	195.6	5.01	695	347	0.2	19.9
CASP22	7.08	221.4	2.83	809	405	0.5	17.71
CASP23	6.98	215.4	5.63	975	487	0	19.42
CASP24	7.12	214.6	6.20	602	301	0.1	18.89

Table S5. Chemical analyses results of groundwater from the fractured aquifer

Code	CAC9	CASP1	CASP4	CASP5	CASP7	CASP14	CASP16	CASP18	CASP25	CASP27
Total Hardness [mg $CaCO_3$/L]	287	332.8	153.5	318.9	287	283	229.2	210	346.8	279
HCO_3^-[mg/L]	530.7	470.92	531.92	387.96	498.98	545.34	524.6	520.94	540.46	314.76
Cl^- [mg/L]	122.3619	19.3493	23.2541	9.9687	14.1304	9.1188	7.486	22.3993	37.0084	3.0388
NO_3^-[mg/L]	21.5084	6.4133	44.5389	12.6993	36.4762	0.078	30.2474	0.1304	56.6389	21.3689
SO_4^{2-}[mg/L]	17.5584	11.6771	23.1943	9.5051	12.0585	11.1777	10.7946	19.1833	11.3923	4.5495
Na^+ [mg/L]	87.5264	23.2456	69.3024	8.7214	35.8201	25.9327	16.4408	33.7331	27.5704	3.5709
K^+ [mg/L]	0.2891	2.2218	0.9452	13.0196	2.0431	1.6176	12.5063	2.1276	1.0849	2.8097
Mg^{2+} [mg/L]	0.5259	6.9555	0.8564	9.4569	6.3543	5.4988	9.1402	2.3542	8.1494	2.4108
Ca^{2+} [mg/L]	17.9955	12.7694	3.3224	6.7281	80.473	15.279	1.6108	9.3196	33.3126	12.6877
Alkalinity [mg $CaCO_3$/L]	435	386	436	318	409	447	430	427	443	258
Total arsenic [mg/L]	0.015	0.016	0.034	0.009	0.016	0.014	0.019	0.019	0.011	0.017
As^{5+} [mg/L]	0.012	0.015	0.03	*	0.013	0.011	0.017	0.015	0.009	0.014
As^{3+} [mg/L]	0.003	0.001	0.004	*	0.003	0.002	0.002	0.004	0.003	0.003
HCO_3^- [meq/L]	8.70	7.72	8.72	6.36	8.18	8.94	8.60	8.54	8.86	5.16
Cl^- [meq/L]	3.45	0.55	0.66	0.28	0.40	0.26	0.21	0.63	1.04	0.09
NO_3^-[meq/L]	0.35	0.10	0.72	0.20	0.59	0.00	0.49	0.00	0.91	0.34
SO_4^{2-}[meq/L]	0.37	0.24	0.48	0.20	0.25	0.23	0.22	0.40	0.24	0.09
Cl^- + NO_3^- [meq/L]	3.79	0.65	1.37	0.49	0.99	0.26	0.70	0.63	1.96	0.43
$\sum$ anions	12.86	8.61	10.58	7.04	9.42	9.43	9.52	9.57	11.05	5.69
Na^+ [meq/L]	3.81	1.01	3.01	0.38	1.56	1.13	0.71	1.47	1.20	0.16
K^+ [meq/L]	0.01	0.06	0.02	0.33	0.05	0.04	0.32	0.05	0.03	0.07
Mg^{2+} [meq/L]	0.04	0.57	0.07	0.78	0.53	0.45	0.76	0.19	0.67	0.20
Ca^{2+} [meq/L]	0.90	0.64	0.17	0.34	4.02	0.76	0.08	0.47	1.67	0.63
Na^+ + K^+ [meq/L]	3.81	1.07	3.04	0.71	1.61	1.17	1.03	1.52	1.23	0.23
$\sum$ cations	4.76	2.28	3.27	1.83	6.16	2.39	1.87	2.18	3.57	1.06
SAR index	5.5	1.3	8.8	0.5	1.0	1.4	1.1	2.6	1.1	0.2
Error (%)	-46.00	-58.12	-58.72	-58.75	-20.92	-59.60	-67.17	-62.88	-51.22	-68.55

*Sample with low levels of total arsenic, so speciation was not performed.

Table S6. Chemical analyses results of groundwater from the sedimentary aquifer

Code	CAC1	CAC2	CAC3	CAC4	CAC6	CAC7	CAC8
Total Hardness [mg $CaCO_3$/L]	221.2	209.3	271	177.4	613.8	181.4	261.1
HCO_3^- [mg/L]	552.66	671	309.88	588.04	549	677.1	367.22
Cl^- [mg/L]	29.782	45.1622	11.2047	66.2156	107.7378	45.0501	6.1998
NO_3^- [mg/L]	60.5547	23.8793	9.5076	0.1254	192.6781	47.7506	13.211
SO_4^{2-} [mg/L]	22.6948	23.0566	9.2158	27.2114	73.9157	40.4666	9.3057
Na^+ [mg/L]	72.939	80.4547	7.0002	30.1274	35.1252	94.944	14.9402
K^+ [mg/L]	2.9267	1.1986	14.0325	13.8217	6.4023	0.5229	4.0278
Mg^{2+} [mg/L]	3.1757	2.8861	10.1916	9.1757	16.0648	0.9222	3.2233
Ca^{2+} [mg/L]	9.6613	4.3861	4.1918	1.2634	10.9569	2.4676	17.3363
Alkalinity [mg $CaCO_3$/L]	453	550	254	482	450	555	301
Total arsenic [mg/L]	0.023	0.021	0.011	0.03	0.014	0.018	0.013
As^{5+} [mg/L]	0.018	0.017	0.009	0.024	0.012	0.014	0.011
As^{3+} [mg/L]	0.005	0.003	0.002	0.006	0.002	0.004	0.002
HCO_3^- [meq/L]	9.06	11.00	5.08	9.64	9.00	11.10	6.02
Cl^- [meq/L]	0.84	1.27	0.32	1.87	3.03	1.27	0.17
NO_3^- [meq/L]	0.98	0.39	0.15	0.00	3.11	0.77	0.21
SO_4^{2-} [meq/L]	0.47	0.48	0.19	0.57	1.54	0.84	0.19
$Cl^- + NO_3^-$ [meq/L]	1.82	1.66	0.47	1.87	6.14	2.04	0.39
$\sum$ anions	11.35	13.14	5.74	12.07	16.68	13.98	6.60
Na^+ [meq/L]	3.17	3.50	0.30	1.31	1.53	4.13	0.65
K^+ [meq/L]	0.07	0.03	0.36	0.35	0.16	0.01	0.10
Mg^{2+} [meq/L]	0.26	0.24	0.84	0.76	1.33	0.08	0.27
Ca^{2+} [meq/L]	0.48	0.22	0.21	0.06	0.55	0.12	0.87
$Na^+ + K^+$ [meq/L]	3.25	3.53	0.66	1.66	1.69	4 .14	0.75
$\sum$ cations	3.99	3.99	1.72	2.48	3.57	4.34	1.89
SAR index	5.2	7.3	0.4	2.0	1.6	13.1	0.9
Error (%)	-47.96	-53.44	-53.99	-65.86	-64.77	-52.62	-55.56

Table S7. Chemical analyses results of groundwater from the sedimentary aquifer (continuation)

Code	CASP2	CASP3	CASP9	CASP10	CASP11	CASP12	CASP13	CASP15
Total Hardness [mg $CaCO_3$/L]	237.2	312.9	312.9	179.5	243.1	269.1	223.2	253.1
HCO_3^- [mg/L]	405.04	529.48	553.88	433.1	418.46	387.96	620.98	359.9
Cl^- [mg/L]	7.0856	39.1887	ND	8.3821	7.0487	3.6785	23.5943	36.5148
NO_3^- [mg/L]	3.3432	11.545	ND	22.9146	6.2061	17.2841	25.7006	31.9906
SO_4^{2-} [mg/L]	10.1368	20.7174	ND	10.7583	15.9682	8.1626	39.4427	28.5169
Na^+ [mg/L]	27.9852	37.3348	107.7754	31.3446	18.172	20.0137	35.4598	26.6857
K^+ [mg/L]	14.0264	4.1253	0.9452	0.1689	14.9291	2.4687	14.9082	16.0384
Mg^{2+} [mg/L]	12.5409	5.9213	6.2522	19.5463	10.6838	3.6676	10.9605	12.1918
Ca^{2+} [mg/L]	13.4325	2.7989	13.3568	3.2412	6.2857	8.857	2.5931	9.1759
Alkalinity [mg $CaCO_3$/L]	332	434	454	355	343	318	509	295
Total arsenic [mg/L]	0.011	0.022	0.014	0.023	0.016	0.009	0.022	0.012
As^{5+} [mg/L]	0.008	0.017	0.011	0.019	0.014	0.008	0.018	0.01
As^{3+} [mg/L]	0.003	0.005	0.003	0.004	0.002	0.001	0.004	0.002
HCO_3^- [meq/L]	6.64	8.68	9.08	7.10	6.86	6.36	10.18	5.90
Cl^- [meq/L]	0.20	1.10	-	0.24	0.20	0.10	0.66	1.03
NO_3^- [meq/L]	0.05	0.19	-	0.37	0.10	0.28	0.41	0.52
SO_4^{2-} [meq/L]	0.21	0.43	-	0.22	0.33	0.17	0.82	0.59
Cl^- + NO_3^-[meq/L]	0.25	1.29	-	0.61	0.30	0.38	1.08	1.54
$\sum$ anions	7.10	10.40	-	7.93	7.49	6.91	12.08	8.04
Na^+ [meq/L]	1.22	1.62	4.69	1.36	0.79	0.87	1.54	1.16
K^+ [meq/L]	0.36	0.11	0.02	0.00	0.38	0.06	0.38	0.41
Mg^{2+} [meq/L]	1.04	0.49	0.52	1.62	0.88	0.30	0.91	1.01
Ca^{2+} [meq/L]	0.67	0.14	0.67	0.16	0.31	0.44	0.13	0.46
Na^+ + K^+ [meq/L]	1.58	1.73	4.71	1.37	1.17	0.93	1.92	1.57
$\sum$ cations	3.28	2.36	5.89	3.14	2.37	1.68	2.96	3.04
SAR index	1.3	2.9	6.1	1.4	1.0	1.4	2.1	1.4
Error (%)	-36.78	-63.04	-	-43.21	-51.95	-60.91	-60.66	-45.16

ND: no detectable

Table S8. Chemical analyses results of groundwater from the sedimentary aquifer (continuation)

Code	CASP17	CASP19	CASP20	CASP21	CASP22	CASP23	CASP24	CASP26
Total Hardness [mg $CaCO_3$/L]	259.7	211.3	165.4	281	474.3	480.3	225.2	374.7
HCO_3^- [mg/L]	367.22	539.24	370.88	387.96	520.94	466.04	309.88	427
Cl^- [mg/L]	7.1156	40.164	10.3855	6.9419	40.9067	ND	14.5666	23.0666
NO_3^- [mg/L]	14.3355	18.9208	19.3179	24.6479	9.639	ND	20.1673	30.0384
SO_4^{2-} [mg/L]	6.8579	31.6574	10.9352	8.6744	26.4654	ND	15.5322	13.7125
Na^+ [mg/L]	13.4274	63.0057	32.4134	94.6597	23.5455	15.9432	12.3549	12.2724
K^+ [mg/L]	2.3875	15.5233	2.4167	0.02	17.3766	13.4635	13.0422	4.3202
Mg^{2+} [mg/L]	1.9205	13.1611	2.4818	0.3217	17.2907	14.2679	9.7082	6.9455
Ca^{2+} [mg/L]	19.9139	7.8744	7.1904	17.8734	32.3182	20.8699	5.0149	14.4971
Alkalinity [mg $CaCO_3$/L]	301	442	304	318	427	382	254	350
Total arsenic [mg/L]	0.006	0.024	0.018	0.021	0.014	0.011	0.017	0.014
As^{5+} [mg/L]	*	0.02	0.015	0.019	0.009	0.008	0.015	0.011
As^{3+} [mg/L]	*	0.004	0.003	0.002	0.005	0.002	0.002	0.003
HCO_3^- [meq/L]	6.02	8.84	6.08	6.36	8.54	7.64	5.08	7.00
Cl^- [meq/L]	0.20	1.13	0.29	0.20	1.15	-	0.41	0.65
NO_3^- [meq/L]	0.23	0.31	0.31	0.40	0.16	-	0.33	0.48
SO_4^{2-} [meq/L]	0.14	0.66	0.23	0.18	0.55	-	0.32	0.29
$Cl^- + NO_3^-$ [meq/L]	0.43	1.44	0.60	0.59	1.31	-	0.74	1.13
$\sum$ anions	6.59	10 94	6.91	7.13	10.40	-	6.14	8.42
Na^+ [meq/L]	0.58	2.74	1.41	4.12	1.02	0.69	0.54	0.53
K^+ [meq/L]	0.06	0.40	0.06	0.00	0.44	0.34	0.33	0.11
Mg^{2+} [meq/L]	0.16	1.09	0.21	0.03	1.43	1.18	0.80	0.57
Ca^{2+} [meq/L]	1.00	0.39	0.36	0.89	1.62	1.04	0.25	0.72
$Na^+ + K^+$ [meq/L]	0.64	3.14	1.47	4.12	1.47	1.04	0.87	0.64
$\sum$ cations	1.80	4.62	2.04	5.04	4.51	3.26	1.92	1.94
SAR index	0.8	3.2	2.7	6.1	0.8	0.7	0.7	0.7
Error (%)	-57.13	-40.62	-54.50	-17.23	-39.47	-	-52.28	-62.50

ND: no detectable; *Sample with low levels of total arsenic, so speciation was not performed.

Table S9. Results of bacteriological analyses of groundwater from the fractured aquifer

	Total coliforms ufc/100 mL	Fecal coliforms ufc/100 mL	*Pseudomonas aeruginosa* ufc/100mL	Heterotrophic bacteria at 35 °C ufc/mL
Methods	APHA 23ª Ed. SM 9222 B	APHA 23ª Ed. SM 9222 D	UNIT 943:1994	FM/APHA 9215 D 2005
Maximum allowed value	<1 ufc/100 mL	<1 ufc/100 mL	<1ufc/100 mL	<= 500 ufc/mL
CAC9	>160	66	<1	>2000
CASP1	>160	52	<1	860
CASP4	>160	<1	<1	410
CASP5	>160	>120	<1	1840
CASP7	104	20	<1	760
CASP14	<1	<1	<1	110
CASP16	<1	<1	>400	440
CASP18	22	<1	<1	310
CASP25	22	2	<1	690
CASP27	>160	2	>400	1900

Source. Strambini Ruiz (2023).

Table S10. Results of bacteriological analyses of groundwater from the sedimentary aquifer

	Total coliforms ufc/100 mL	**Fecal coliforms ufc/100 mL**	***Pseudomonas aeruginosa* ufc/100mL**	**Heterotrophic bacteria at 35 °C ufc/mL**
Methods	APHA 23ª Ed. SM 9222 B	APHA 23ª Ed. SM 9222 D	UNIT 943:1994	FM/APHA 9215 D 2005
Maximum allowed value	<1 ufc/100 mL	<1 ufc/100 mL	<1ufc/100 mL	<= 500 ufc/mL
CAC1	>160	<1	<1	>2000
CAC2	>160	118	<1	>2000
CAC3	24	<1	<1	>2000
CAC4	<1	<1	<1	1800
CAC6	>160	36	<1	1720
CAC7	>160	<1	<1	910
CAC8	>160	>120	<1	390
CASP2	<1	<1	22	660
CASP3	>160	<1	<1	>2000
CASP9	>160	<1	<1	>2000
CASP10	<1	<1	54	1620
CASP12	>160	38	<1	1670
CASP13	>160	16	<1	1190
CASP15	<1	<1	<1	390
CASP17	>160	24	<1	400
CASP19	<1	<1	<1	70
CASP20	8	<1	18	290
CASP21	<1	<1	<1	50
CASP22	>160	>120	<1	910
CASP23	<1	<1	<1	100
CASP24	<1	<1	<1	50
CASP26	34	<1	<1	2000

Source. Strambini Ruiz (2023).